Scientific Research Publishing

Open Journal of Geology, 2023, 13, 536-578
https://www.scirp.org/journal/ojg
ISSN Online: 2161-7589
ISSN Print: 2161-7570

Paleostress Reconstruction from 3D Seismic Data and Slip Tendency in the Northern Slope Area of the Bongor Basin, Southwestern Chad

Hakro Ahmed Suhail[1*], Xintao Yuan[2,3], Jianlin Li[1], Hong Liu[1], Yuan Liu[1], Cong Ma[1]

[1]Geophysical Research Institute, BGP/CNPC, Hebei, China
[2]CNPC International (Chad) Co., Ltd., N'Djamena, Chad
[3]Research Institute of Petroleum Exploration and Development, Beijing, China
Email: *ahmed1985@cnpc.com.cn

How to cite this paper: Suhail, H.A., Yuan, X.T., Li, J.L., Liu, H., Liu, Y. and Ma, C. (2023) Paleostress Reconstruction from 3D Seismic Data and Slip Tendency in the Northern Slope Area of the Bongor Basin, Southwestern Chad. *Open Journal of Geology*, **13**, 536-578.
https://doi.org/10.4236/ojg.2023.135024

Received: April 17, 2023
Accepted: May 28, 2023
Published: May 31, 2023

Abstract

Paleostress plays a significant role in controlling the formation, accumulation, and distribution of reservoirs, and this could be an important factor in controlling the production of hydrocarbons from the unconventional reservoirs. In this study, we will use 3D seismic reflection data to perform the slip-tendency-based stress inversion to determine the stress field in the basement of the northern slope area in the Bongor Basin. The dataset for this technique is easily available in the oil and gas companies. The stress inversion results from the basement of the northern slope area of Bongor basin show that the maximum principal stress axis ($\sigma 1$) is oriented vertically, the intermediate principal stress axis ($\sigma 2$) is oriented N18˚ and the minimum principal stress axis ($\sigma 3$) is oriented N105˚, and $\sigma 2/\sigma 1 = 0.60$ and $\sigma 3/\sigma 1 = 0.29$. The findings of this paper provide significant information to understand the fault reactivation at the critical stage of hydrocarbon accumulation and the regional tectonic evolution.

Keywords

Seismic Reflection Data, Slip Tendency, Bongor Basin, Stress Inversion

1. Introduction

Faults and fractures are significant factors in subsurface fluid current in complex geological structures [1]. Fault reactivation is a hot topic in the development of reservoirs [2], and natural fractures are employed to anticipate the favorable zone for oil and gas exploration [3] [4] [5] [6] [7]. In general, both faults and fractures are considered to be fractures [8]. During the tectonic evolution, rocks

may have been experienced a wide range of stress magnitude and orientations, the resulting in rock failure and fractures; thus, the reconstruction of the paleostress plays an important role in precise fracture prediction. In addition, paleostress reconstruction is a crucial approach for studying a region's tectonic evolution [9]-[21]. Paleostress field investigation is useful to explain fault reactivation [22] [23], and the timing and designs of fault leakage [22] [23] [24] [25]. Nowadays, a couple of methods have been proposed for estimating Paleostress analysis, such as earthquake focal mechanisms [26], fault-slip data inversion [27]-[34]. However, these techniques are based on the outcrops and oriented core data. Such data is not easily available in the petroleum companies. Geologists are frequently concerned about the subsurface geological structures, and the data can be easily obtained from the 3D seismic interpretation, which usually does not relate to the field outcrop data.

In this paper, we will use the stress inversion method based on 3D seismic interpretation data, and slip tendency analysis. The method was used to reconstruct the Paleostress tensor in the basement of the northern Slope area of the Bongor Basin. The inversion results can be used to examine regional tectonic evolutions and are an important source of information for determining fault reactivity at the critical stage in the hydrocarbon accumulation.

2. Background of the Study Area

The Bongor Basin is located in the southwestern Chad, north of the middle section of the Central African Shear Zone (CASZ) (**Figure 1(a)**). On the other hand, this basin is an intracontinental rift basin that formed throughout the Mesozoic and Cenozoic under the influence of the (CASZ). The formation and evolution of this basin are closely related to the evolution of the African Plate, especially the shear zone in Central and West Africa, with typical passive rift characteristics [35] [36]. The Bongor basin covers an area of approximately 18,000 km^2. From east to west, this Basin extends for ~280 km long and 40 - 80 km wide, and is divided into four structural units based on the Bouguer gravity, aeromagnetic, and seismic data: the northern slope, central sub-basin, southern sub-basin, and southern uplift (**Figure 1(b)**) [37]. The central sub-basin is further separated into four depressions Annona Depression, Cola Depression, Mango Depression, and Moul Depression.

The basement of the Bongor basin is composed of Precambrian metamorphic rock, similar to the basement of the Sudan Rift Basin in nature [38] [39] [40], on which tens of thousands of meters of Mesozoic and Cenozoic continental clastic rock strata are deposited, including the Lower Cretaceous, Tertiary, and Quaternary (**Figure 2**). According to the characteristics of gravity, aeromagnetic and seismic reflection wave groups and the distribution of regional unconformity, the sedimentary cover in the basin is further divided into two major structural layers: the Lower Cretaceous and the Cenozoic. These structural layers reflect that the tectonic evolution of the Bongor Basin underwent major rift activity,

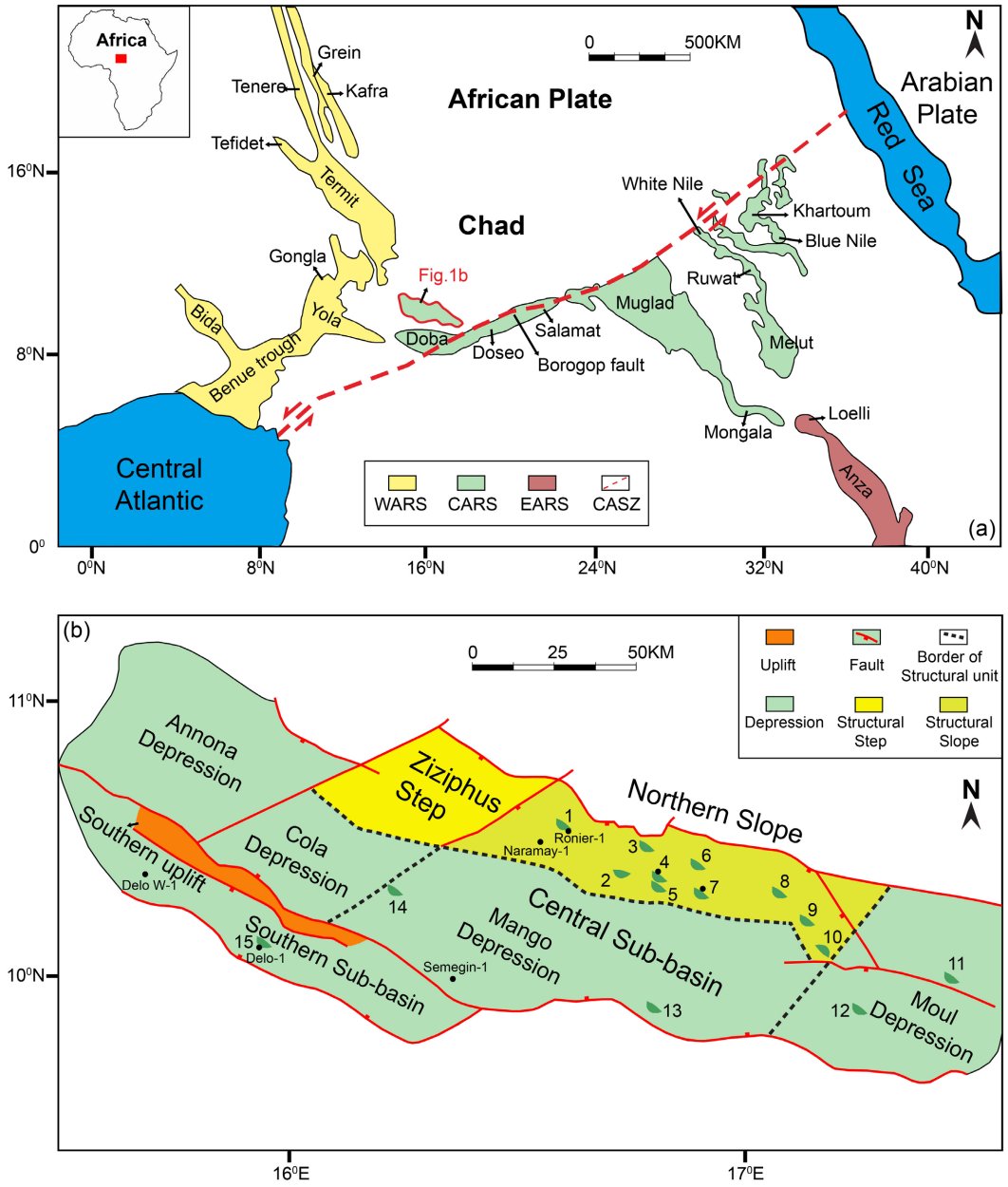

Figure 1. Location map of study area (b) Simplified structural map of the Bongor basin. Modified after [37]. Oil/gas fields: 1-Ronier; 2-Mimosa; 3-Baobab; 4-Phoenix; 5-Phoenix S; 6-Raphia S-8; 7-Raphia S-6; 8-Daniela; 9-Lanea; 10-Lanea E; 11-Pavetta; 12-Moul; 13-Mango; 14-Vitex; 15-Delo. WARS: West African Rift System; CARS: Central African Rift System; EARS: East African Rift System; CASZ: Central African Shear Zone.

strong inversion, and a subsequent depression subsidence stage. The lower Cretaceous is the main period for the development of the rift, during which the main source and reservoir rock of the basin were deposited. During the lower Cretaceous, Bongor Basin underwent rapid subsidence in the early (Prosopis and Mimosa Formation sedimentary periods) and slow subsidence in the late (Kabula and Baobab Formation sedimentary periods) stages. About 85 - 80 Ma ago, the Santonian compression event was caused by the collision of the African and the Eurasian plate.

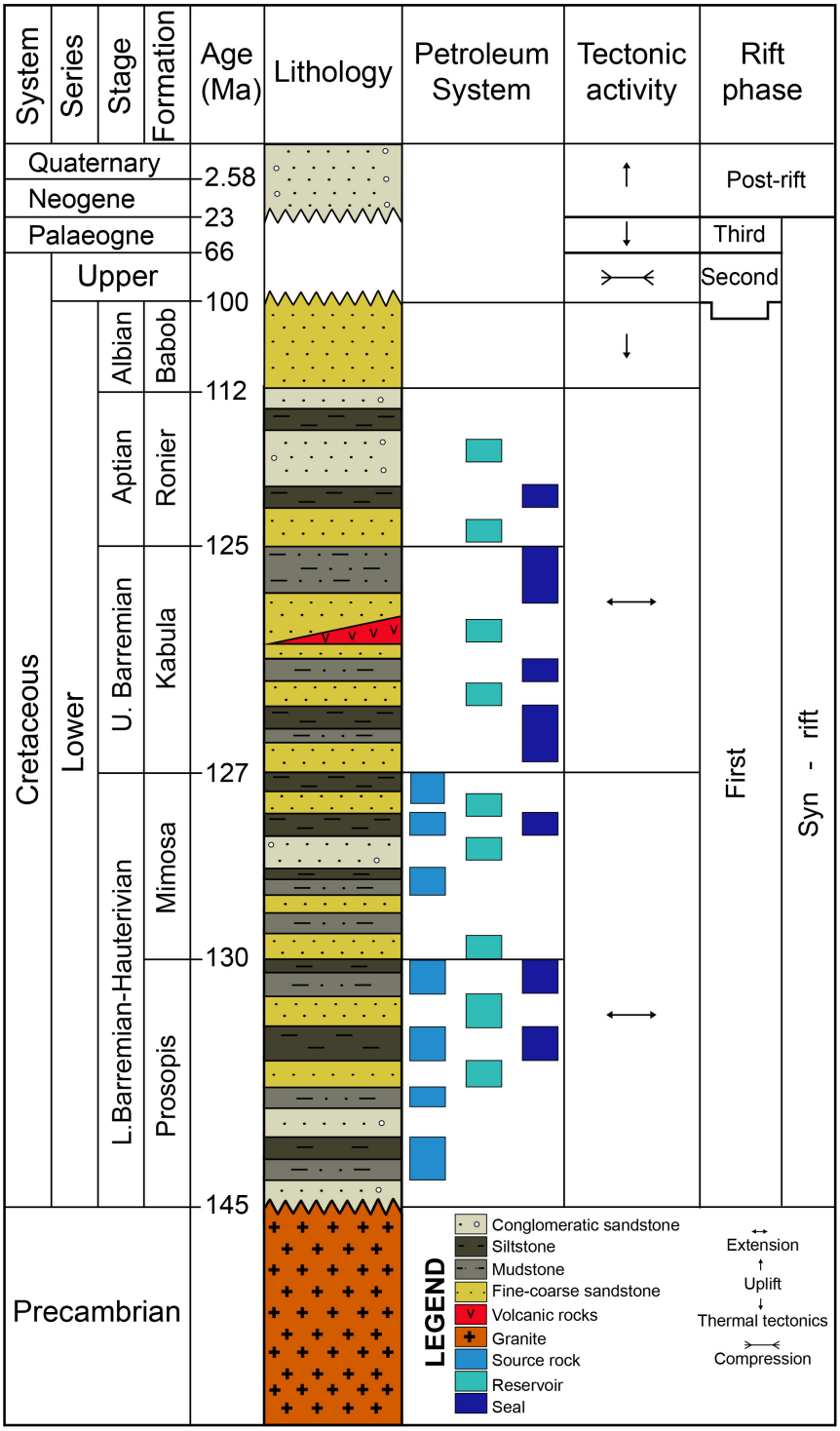

Figure 2. Regional stratigraphy of the Bongor basin showing the petroleum system and tectonic phases. Modified after [47].

The reversal event, especially in the Bongor Basin is very strong, with the overall uplift of the basin being strong in the west and weak in the east, resulting in a lack of Upper Cretaceous in the basin. Entering the Cenozoic era, the regional stress field underwent significant changes, exhibiting strong extension in

the West African Rift System and Sudan region, while thermal subsidence was dominant in the Bongor Basin. Correspondingly, the Termit Basin of the West African Rift System experienced strong subsidence, with a thickness of 3000 meters in the Tertiary strata, while the Bongor Basin had a maximum thickness of fewer than 500 meters in the Tertiary sediments. Therefore, the reservoir formation conditions of the Bongor Basin are similar to the basins of the West African Rift (WAR) and Sudan. There are significant differences between the Muglad Basin and the Melut Basin, as well as the Doba Basin in southern Chad.

The Bongor Basin is dominated by half-graben structures. Main boundary faults are generally striking in the ENE or WSW (**Figure 3**) and the dip angle of boundary faults and major faults varies from 30˚ to 50˚ but is most prominent at 45˚ in the SE and NW. The structural style in the Bongor basin is the large-scale domino fault blocks formed during the lower Cretaceous expansion and the transpressional inversion anticlines that formed on the hanging wall. The extensional topography has been intact; however, there has been an uplift of around 1500 m, with an 8% shortening ratio for the entire basin and, 20% for the half-grabens of the northern slope. A locally or regionally inverted rift basin would be a good way to describe the Bongor basin [41] [42] with various inversion styles and intensities in different regions of the basin.

3. Methodology

3.1. Slip Tendency Analysis

The idea behind slip tendency analysis is that the resolved shear stress and normal stress on a surface are excellent predictors of both the likelihood and the slip direction on the surface [43]. The approach has been used successfully to define fault slip and fault directions [44] [45] [46]. High slip-tendency oriented fractures are frequently more effective flow conduits than low slip-tendency orientation fractures [1] [43] [47] [48]. Stress anisotropy has the greatest impact when a

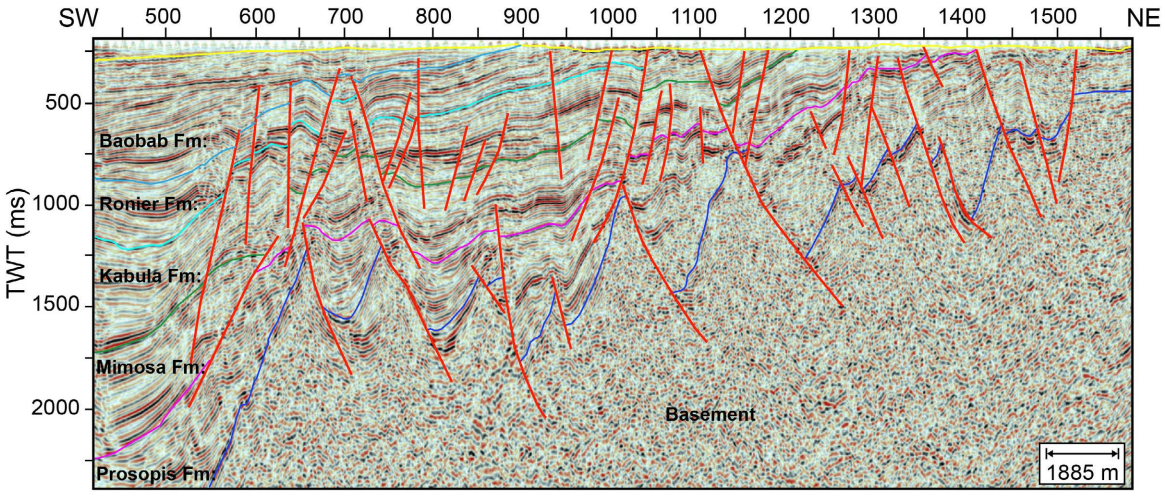

Figure 3. Seismic section illustrating the fault characteristic in the study area, location of seismic section shown in **Figure 4**.

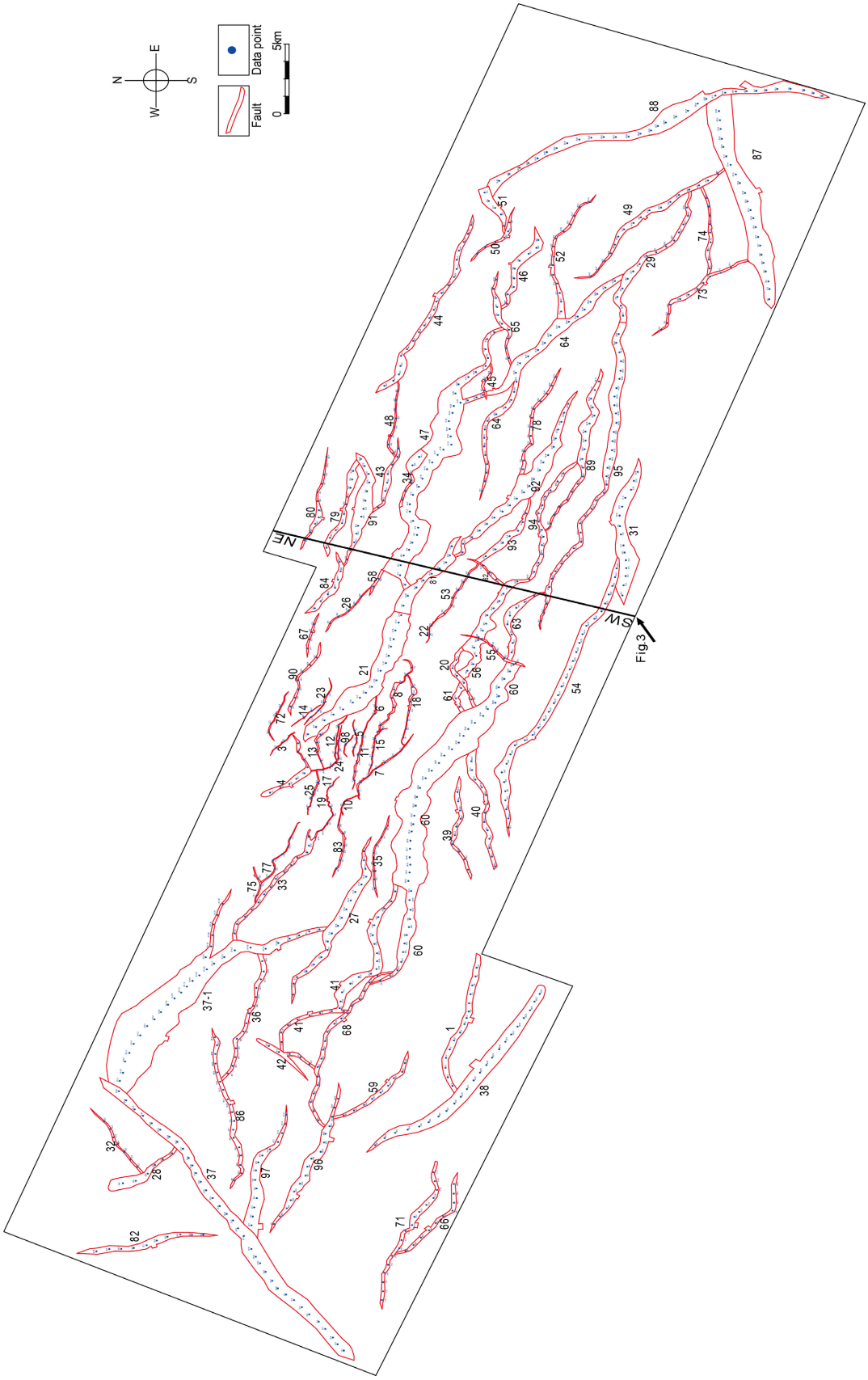

Figure 4. Structural map of the basement of the northern slope of Bongor basin.

crack or fracture's effective stress conditions are close to those needed for slip [49] [50] [51]. However, preferential fluid flow in fault and fracture routes becomes more obvious when the differential stress increases and the region of both faults and fractures with higher slip propensity increases [1] [43] [52] [53].

In general, Equation (1) defines the slip tendency (Ts) of a fault as the shear stress (τ) to the normal stress (σn) on the surface [43]:

$$Ts = \frac{\tau}{\sigma n} \tag{1}$$

In this study, we derived the equation of extensional regimes. For example, there are three principal stresses $\sigma 1 > \sigma 2 > \sigma 3$ in space, the Anderson model suggests, there is a major stress axis that is perpendicular to the ground since the Earth's surface is a principal stress plane.

In the extensional deformation regimes, the maximum principal stress axis ($\sigma 1$) is oriented vertically, and the intermediate principal stress axis ($\sigma 2$) and minimum principal stress axis ($\sigma 3$) are horizontal. The estimate of stress tensor (maximum a posteriori (MAP) is also known as the maximum likelihood and least squares estimations. The relative magnitude of the principal stresses is for the numerical best-fit stress tensor.

These parameters are determined using a 3D stress computer program developed by the Southwest Research Institute (SWRI). The stress regime is defined by the nature of the vertical stress axes:

1) Extensional stress regime when $\sigma 2$ is the maximum horizontal stress axis and $\sigma 1$ is vertical.

2) Strike-slip stress regime when $\sigma 1$ is the maximum horizontal stress and $\sigma 2$ is vertical.

3) Compressional stress regime when $\sigma 1$ is the maximum horizontal stress $\sigma 3$ is vertical.

3.2. Slip Tendency-Based Stress Inversion

The slip tendency values can be used to calculate the likelihood and the fault slip direction on the fault surface. A higher slip tendency indicates the fault is more likely to reactivate, and that there will be more sliding along the fault with respect to time. Therefore, faults with higher slip tendency values accure a larger fault displacement than faults with lower slip tendency. However, there are a few exceptions, there is a fault with a higher slip tendency and slips during the end of the deformation history. As a result, a wide range of fault displacement values could be found in the faults with higher slip tendency. Therefore, the slip tendency can be used as a proxy for fault displacement [54].

The stress inversion method characterized the degree of agreement between the computed slip tendency values of the stress tensor and the measured displacement values for a set of observed surfaces. In order to assess a candidate stress tensor's ability to explain the pattern of displacement on the surface of different variable [43].

4. Results

4.1. Data

The northern slope of the Bongor Basin covers an area of ~3200 km^2. 3D data for the whole area is available. The original data has been well processed; the seismic volume's linear spacing is 25 m, the primary frequency is 15 - 30 Hz, and it has been loaded to a workstation and interpreted using GeoEast v.3.3.1. The structural maps of the basement (Figure 4) obtained from the time-depth conversion of 3D seismic interpretation data.

The geometric parameters of fault strike, dip angle and displacement in the basement were measured through 3D seismic interpretation. A total of n = 1123 fault data points were collected from the basement (Figure 4 and Table S1).

Fault Displacement was calculated from the seismic sections that were orthogonal to the direction of the adjacent fault. The horizontal and vertical distances between the footwall and hanging wall were used to compute the fault displacement.

A stereographic projection of faults with various displacement values is shown in Figure 5. The stereographic projection shows that the strike of the fault with larger displacement is in the NE-SW direction, but we can find some lower displacement values in the NW-SE direction, which could be the impact of the pre-existing fault structure in the basement. In general, high-angle faults typically accumulated higher displacement and are easier to reactivate. However, faults with the lower displacement are distributed in the SE-NW (Figure 5).

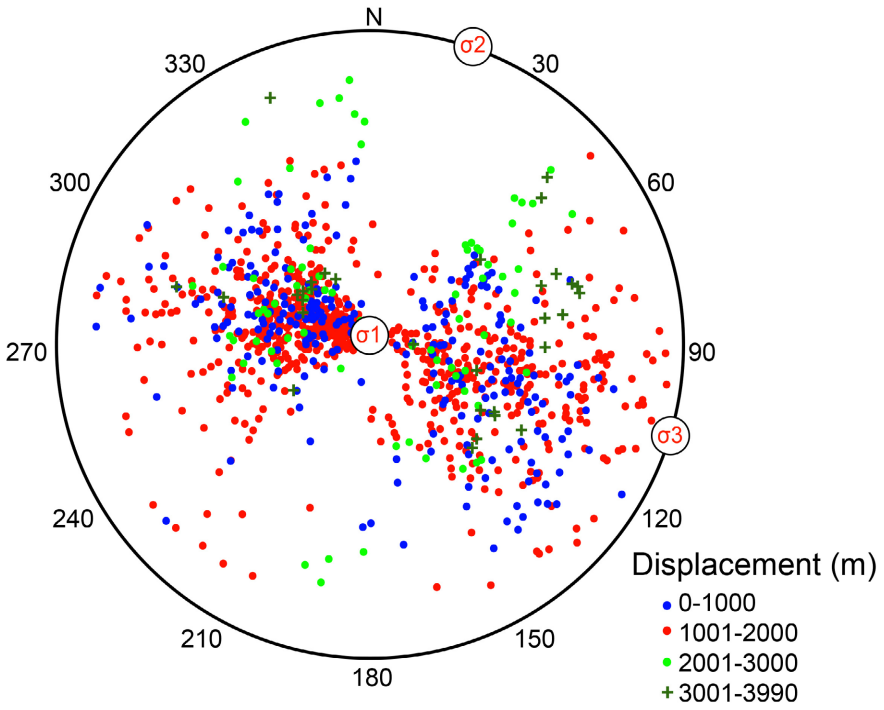

Figure 5. Fault displacement of basement. Stereographic projection (lower hemisphere, Schmidt projection) with fault poles.

4.2. Stress Inversion Results

A total of n = 1123 fault points were measured from the basement. The fault geometric parameters, *i.e.* strike, dip, and displacement which were obtained from the 3D seismic interpretation data to acquire the stress state condition under the slip tendency. In order to analyze this particular dataset, no artificial data are required. Table 1, describes the stress tensor's maximum a posteriori (MAP) estimation.

The maximum and minimum slip tendency values in the data were recorded in 3D stress. Slip tendency results show in (Figure 6). For each fault point's the fault displacement and slip tendency values were normalized [53]. The slip tendency values ranged from 0 to 1 allowing a direct comparison of the slip tendency and fault displacement. The Paleostress inversion determines the slip tendency that best corresponds to the fault displacement. The final stress inversion results show that the maximum principal stress axis $\sigma 1$ is oriented vertically, the intermediate principal stress axis $\sigma 2$ is oriented N18˚ and minimum principal stress axis $\sigma 3$ is oriented N105˚, and $\sigma 2/\sigma 1$ = 0.60 and $\sigma 3/\sigma 1$ = 0.29.

Table 1. MAP Stress tensor estimate of basement.

Principal stress	Magnitude	Plunge (˚)	Azimuth (˚)
$\sigma 1$	353.6	90˚	23.08˚
$\sigma 2$	199	0.4˚	13.85˚
$\sigma 3$	288	−0.2˚	6.92˚

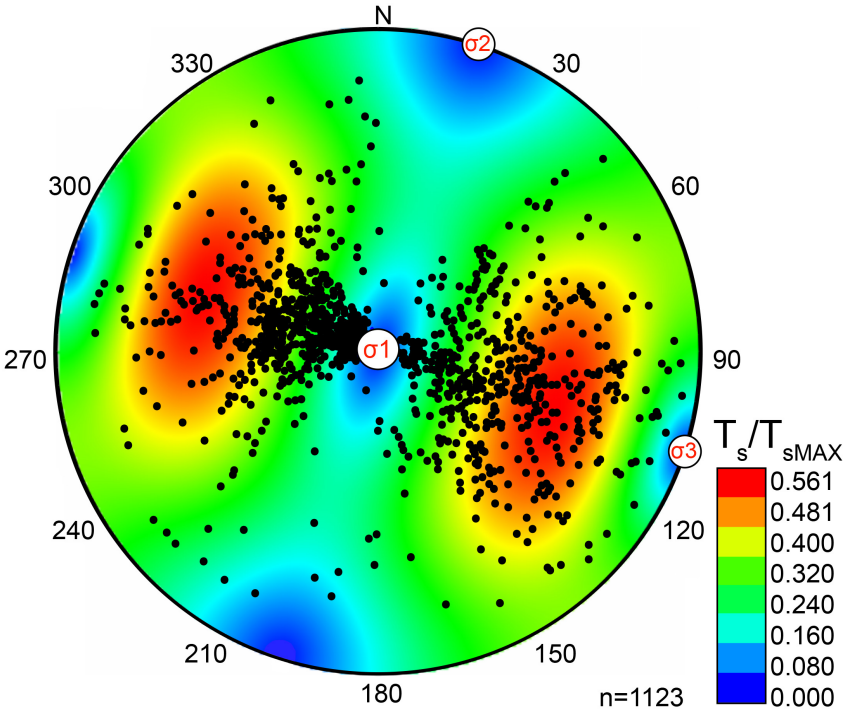

Figure 6. Principal stress orientation and slip tendency plot of the basement of the northern slope area of the Bongor basin.

5. Discussion

In order to keep the production from the unconventional reservoir. Paleostress plays an important role in controlling and distributing of fractured reservoirs. Nowadays, couples of methods to invert Paleostress, but these methods are still dependent on the outcrop or oriented core data. Those data are generally not available in the oil and gas companies. The slip tendency-based stress inversion approach was previously demonstrated mainly by outcrop data [34] but it hasn't been used with the seismic reflection data. Previously 3D seismic reflection data was used by [55] to perform the slip tendency based stress inversion through the slip tendency algorithm presented by [54] to identify the stress field of the Xicaogu area in the Bohai Bay Basin. However, we used the 3D Stress software package by the SWRI to perform the Slip tendency-based stress inversion to infer the stress field in the basement of the northern slope area in the Bongor basin. This method is based on the slip tendency and fault displacement and the dataset for this method can be easily collected from the oil and gas companies.

The stress inversion was accomplished based on the fault geometric data obtained from the seismic interpretation data. The fault surface orientation and displacement in the basement of the northern slope area of the Bongor basin were examined. The result shows that the fault displacements of each fault point exist in different areas of the stereographic projection and the faults with higher displacement values, steeper dip angle, and high slip tendency values are easier to reactivate than those faults with low slip tendency and displacement. This relationship provides a fault displacement that can be used as a proxy for slip tendency.

The stress state that best matched the slip tendency values and the fault displacement of the observed surface, the stress inversion was achieved based on the fault geometric data obtained from the 3D seismic interpretation data. The Paleostress inversion results show that the slip tendency has been found especially in the NE-SW direction.

Different stages of evolution were thought to have occurred in the Bongor Basin: a basement-forming period, and a strong setting period in the lower Cretaceous Prosopis and Mimosa formations. A Stable setting period in the lower Cretaceous Kabula, Ronier, and Baobab formation, and thermal precipitation during the Cenozoic. The Cretaceous rifting and Neogene post-rifting thermal subsidence were thought to have occurred in the Bongor Basin. The basin strike-slip regime is characterized by the west-northwest, east-southeast striking faults; these faults primarily controlled the deposition of lower Cretaceous sediments in the Bongor Basin, indicating that the faults may have been related to pre-existing basement faults and reactivated during the lower Cretaceous. This phenomenon might be connected to the basement faults reactivating as a result of the strike-slip movement of the Central African Shear Zone. The cumulative fault displacement during the tectonic or stress event was different, but the slip could accumulate on randomly oriented, potentially pre-existing faults.

The slip tendency-based stress inversion method opens a new and intriguing view point on paleostress analysis. Some modern software, such as Trap Tester, Move Midland Valley, can also be used to estimate the paleostress. This method is currently undergoing additional development and testing.

6. Conclusion

Based on the fault geometrics and displacement obtained from the 3D seismic interpretation data, stress inversion was then obtained by determining the stress state that best matched with the slip tendency values and the displacement of measures surface. The Paleostress inversion results show that the maximum principal stress axis ($\sigma 1$) is oriented vertically, the intermediate principal stress axis ($\sigma 2$) is oriented N18˚, the minimum principal stress axis and, ($\sigma 3$) is oriented N105˚, and $\sigma 2/\sigma 1 = 0.60$ and $\sigma 3/\sigma 1 = 0.29$. The results show a strong correlation, indicating that most of the faults trend towards the northeast and southwest on the northern slope of the Bongor Basin, and could be related to pre-existing basement faults that were reactivated in the lower Cretaceous because of the strike-slip movement of the Central African Shear Zone.

Acknowledgements

This research work was supported by the China National Petroleum Corporation (No. CNPCIC-CT-2002-008).

Declaration of Competing Interest

The authors declare that they have no known competing financial interests or personal relationships that could have appeared to influence the work reported in this paper.

Author Contributions

H.S.; X.Y.; contribute to conception and design of the paper. J.L.; contributes to program, H.L.; analyze the fault kinematics. Y.L.; C.M.; contribute to seismic interpretation. All authors contributed to manuscript revision, read and approved the submitted version.

Conflicts of Interest

The authors declare no conflicts of interest regarding the publication of this paper.

References

[1] Ferrill, D.A., Winterle, J., Wittmeyer, G., Sims, D., Colton, S., Armstrong, A. and Morris, A. (1999) Stressed Rock Strains Groundwater at Yucca Mountain, Nevada. *GSA Today*, **9**, 1-7.

[2] Moeck, I., Kwiatek, G. and Zimmermann, G. (2009) Slip Tendency Analysis, Fault Reactivation Potential and Induced Seismicity in a Deep Geothermal Reservoir.

Journal of Structural Geology, **31**, 1174-1182.
https://doi.org/10.1016/j.jsg.2009.06.012

[3] Magoon, L.B. and Dow, W. (1994) The Petroleum System—From Source to Trap. American Association of Petroleum Geologists, Tulsa.
https://doi.org/10.1306/M60585

[4] Jia, C., Zheng, M. and Zhang, Y. (2012) Unconventional Hydrocarbon Resources in China and the Prospect of Exploration and Development. *Petroleum Exploration and Development*, **39**, 139-146. https://doi.org/10.1016/S1876-3804(12)60026-3

[5] Wang, W., Pang, X., Chen, Z., Chen, D., Zheng, T., Luo, B., Li, J. and Yu, R. (2019) Quantitative Prediction of Oil and Gas Prospects of the Sinian-Lower Paleozoic in the Sichuan Basin in Central China. *Energy*, **174**, 861-872.
https://doi.org/10.1016/j.energy.2019.03.018

[6] Gong, L., Wang, J., Gao, S., Fu, X., Liu, B., Miao, F., Zhou, X. and Meng, Q. (2021) Characterization, Controlling Factors and Evolution of Fracture Effectiveness in Shale Oil Reservoirs. *Journal of Petroleum Science and Engineering*, **203**, Article ID: 108655. https://doi.org/10.1016/j.petrol.2021.108655

[7] Zhang, L., Pang, X., Pang, H., Huo, X., Ma, K. and Huang, S. (2022) Hydrocarbon Accumulation Model Based on Threshold Combination Control and Favorable Zone Prediction for the Lower Enping Formation, Southern Lufeng Sag. *Advances in Geo-Energy Research*, **6**, 438-450. https://doi.org/10.46690/ager.2022.05.08

[8] Li, H., Yu, F., Wang, M., Wang, Y. and Liu, Y. (2022) Quantitative Prediction of Structural Fractures in the Paleocene Lower Wenchang Formation Reservoir of the Lufeng Depression. *Advances in Geo-Energy Research*, **6**, 375-387.
https://doi.org/10.46690/ager.2022.05.03

[9] Jamison, W.R. (1992) Stress Controls on Fold Thrust Style. In: McClay, K.R., Ed., *Thrust Tectonics*, Springer, Berlin, 155-164.
https://doi.org/10.1007/978-94-011-3066-0_13

[10] Van Der Pluijm, B.A., Craddock, J.P., Graham, B.R. and Harris, J.H. (1997) Paleostress in Cratonic North America: Implications for Deformation of Continental Interiors. *Science*, **277**, 794-796. https://doi.org/10.1126/science.277.5327.794

[11] Zain Eldeen, U., Delvaux, U. and Jacobs, P. (2002) Tectonic Evolution in the Wadi Araba Segment of the Dead Sea Rift, South-West Jordan. *EGU Stephan Mueller Special Publication Series*, **2**, 63-80. https://doi.org/10.5194/smsps-2-63-2002

[12] Rowland, S.M., Duebendorfer, E.M. and Schiefelbein, I.M. (2007) Structural Analysis & Synthesis: A Laboratory Course in Structural Geology. 4th Edition, Wiley-Blackwell, Hoboken.

[13] Soumaya, A., Ben Ayed, N., Rajabi, M., Meghraoui, M., Delvaux, D., Kadri, A., Ziegler, M., Maouche, S. and Braham, A. (2018) Active Faulting Geometry and Stress Pattern near Complex Strike-Slip Systems along the Maghreb Region: Constraints on Active Convergence in the Western Mediterranean. *Tectonics*, **37**, 3148-3173.
https://doi.org/10.1029/2018TC004983

[14] Dasgupta, A., Mukherjee, S., Vanik, N., Chatterjee, R. and Pal, S.K. (2023) Paleostress Analyses and Oblique Rift Kinematics of Barmer Rift Basin, Western Rajasthan, India. *Marine and Petroleum Geology*. (Submitted)

[15] Kumar, A., Shaikh, M.A., Singh, S., Singh. T., Mukherjee, S. and Singh, S. (2022) Active Morphogenic Faulting and Paleostress Analyses from the Central Nahan Salient, NW Siwalik Himalaya. *International Journal of Earth Sciences*, **111**, 1251-1267.
https://doi.org/10.1007/s00531-022-02176-3

[16] Biswas, T., Bose, N., Dutta, D. and Mukherjee, S. (2022) Arc-Parallel Shears in Col-

lisional Orogens: Global Review and Paleostress Analyses from the NW Lesser Himalayan Sequence (Garhwal Region, Uttarakhand, India). *Marine and Petroleum Geology*, **138**, Article ID: 105530. https://doi.org/10.1016/j.marpetgeo.2022.105530

[17] Maurya, D.M., Shaikh, M.A. and Mukherjee, S. (2021) Comment on Structural Attributes and Paleostress Analysis of Quaternary Landforms along the Vigodi Fault (VF) in Western Kachchh Region. *Quaternary International*, **601**, 143-147. https://doi.org/10.1016/j.quaint.2021.04.029

[18] Misra, A.A., Bhattacharya, G., Mukherjee, S. and Bose, N. (2014) Near N-S Paleo-Extension in the Western Deccan Region in India: Does It Link Strike-Slip Tectonics with India-Seychelles Rifting? *International Journal of Earth Sciences*, **103**, 1645-1680. https://doi.org/10.1007/s00531-014-1021-x

[19] Dutta, D., Biswas, T. and Mukherjee, S. (2019) Arc-Parallel Compression in the NW Himalaya: Evidence from Structural and Palaeostress Studies of Brittle Deformation from the Clasts of the Upper Siwalik, Uttarakhand, India. *Journal of Earth System Science*, **128**, 125. https://doi.org/10.1007/s12040-019-1138-1

[20] Goswami, T. K., Gogoi, M., Mahanta, B.N., Mukherjee, S., Saikia, H., Shaikh, M.A., Kalita, P., Baral, U. and Sarmah, R.K. (2022) Brittle Tectonics in the Western Arunachal Frontal Fold Belt, India: Change in Stress Regime from Pre-Collisional Extension to Collisional Compression. *Geological Journal*, **57**, 5019-5038. https://doi.org/10.1002/gj.4393

[21] Shaikh, M.A., Maurya, D.M., Mukherjee, S., Vanik, N., Padmalal, A. and Chamyal, L. (2020) Tectonic Evolution of the Intra-Uplift Vigodi-Gugriana-Khirasra-Netra Fault System in the Seismically Active Kachchh Rift Basin, India: Implications for the Western Continental Margin of the Indian Plate. *Journal of Structural Geology*, **140**, Article ID: 104124. https://doi.org/10.1016/j.jsg.2020.104124

[22] Gartell, A.P. and Lisk, M. (2005) Potential New Method for Paleostress Estimation by Combining Three-Dimensional Fault Restoration and Fault Slip Inversion Techniques: First Test on the Skua Field, Timor Sea. In: Boult, P. and Kaldi, J., Eds., *Evaluating Fault and Cap Rock Seals*, AAPG Hedberg Series, No. 2, American Association of Petroleum Geologists, Tulsa, 23-26.

[23] Kulikowski, D. and Amrouch, K. (2018) 4D Modelling of Fault Reactivation Using Complete Paleostress Tensors from the Cooper-Eromanga Basin, Australia. *Australian Journal of Earth Sciences*, **65**, 661-681. https://doi.org/10.1080/08120099.2018.1465472

[24] Du Rouchet, J. (1981) Stress Fields, a Key to Oil Migration. *American Association of Petroleum Geologists Bulletin*, **65**, 74-85. https://doi.org/10.1306/2F919774-16CE-11D7-8645000102C1865D

[25] Henk, A. (2005) Pre-Drilling Prediction of the Tectonic Stress Field with Geomechanical Models. *First Break*, **23**, 53-57. https://doi.org/10.3997/1365-2397.2005021

[26] Gephart, J.W. and Forsyth, D.W. (1984) An Improved Method for Determining the Regional Stress Tensor Using Earthquake Focal Mechanism Data: Application to the San Fernando Earthquake Sequence. *Journal of Geophysical Research*, **89**, 9305-9320. https://doi.org/10.1029/JB089iB11p09305

[27] Etchecopar, A., Vasseur, G. and Daignieres, M. (1981) An Inverse Problem in Microtectonics for the Determination of Stress Tensors from Fault Striation Analysis. *Journal of Structural Geology*, **3**, 51-65. https://doi.org/10.1016/0191-8141(81)90056-0

[28] Angelier, J. (1984) Tectonic Analysis of Fault Slip Data Sets. *Journal of Geophysical Research*, **89**, 5835-5848. https://doi.org/10.1029/JB089iB07p05835

[29] Célérier, B. (1988) How Much Does Slip on a Reactivated Fault Plane Constrain the Stress Tensor? *Tectonics*, **7**, 1257-1278. https://doi.org/10.1029/TC007i006p01257

[30] Yamaji, A. (2000) The Multiple Inverse Method: A New Technique to Separate Stresses from Heterogeneous Fault-Slip Data. *Journal of Structural Geology*, **22**, 441-452. https://doi.org/10.1016/S0191-8141(99)00163-7

[31] Tezuka, K. and Niitsuma, H. (2000) Stress Estimated Using Microseismic Clusters and Its Relationship to the Fracture System of the Hijiori Hot Dry Rock Reservoir. *Engineering Geology*, **56**, 47-62. https://doi.org/10.1016/S0013-7952(99)00133-7

[32] Žalohar, J. and Vrabec, M. (2010) Kinematics and Dynamics of Fault Reactivation: The Cosserat Approach. *Journal of Structural Geology*, **32**, 15-27. https://doi.org/10.1016/j.jsg.2009.06.008

[33] Hansen, J.A. (2013) Direct Inversion of Stress, Strain or Strain Rate Including Vorticity: A Linear Method of Homogenous Fault-Slip Data Inversion Independent of Adopted Hypothesis. *Journal of Structural Geology*, **51**, 3-13. https://doi.org/10.1016/j.jsg.2013.03.014

[34] Tiwari, S.K., Beniest, A. and Biswal, T.K. (2020) Extension Driven Brittle Exhumation of the Lower-Middle Crustal Rocks, a Paleostress Reconstruction of the Neoproterozoic Ambaji Granulite, NW India. *Journal of Asian Earth Sciences*, **195**, Article ID: 104341. https://doi.org/10.1016/j.jseaes.2020.104341

[35] Guiraud, R. and Maurin, J.C. (1992) Early Cretaceous Rifts of Western and Central Africa: An Overview. *Tectonophysics*, **213**, 153-168. https://doi.org/10.1016/0040-1951(92)90256-6

[36] Genik, G.J. (1992) Regional Framework, Structural and Petroleum Aspects of Rift Basins in Niger, Chad and the Central African Republic (C.A.R.). In: Ziegler, P.A., Ed., *Geodynamics of Rifting*, Elsevier, Amsterdam, 169-185. https://doi.org/10.1016/B978-0-444-89912-5.50036-3

[37] Dou, L., Xiao, K., Hu, Y., Song, H., Cheng, D. and Du, Y. (2011) Petroleum Geology and a Model of Hydrocarbon Accumulations in the Bongor Basin, the Republic of Chad. *Acta Petrolei Sinica*, **32**, 379-386.

[38] Tong, X.G., Dou, L., Tian, Z.J., Pan, X.H. and Zhu, X.D. (2004) Geological Mode and Hydrocarbon Accumulation Mode in Muglad Passive Rift Basin of Sudan. *Acta Petrolei Sinica*, **25**, 19-24.

[39] Tong, X.G., Xu, Z., Shi, B., Dou, L. and Xiao, K. (2006) Petroleum Geologic Property and Reservoir-Forming Pattern of Melut Basin in Sudan. *Acta Petrolei Sinica*, **27**, 1-5.

[40] Dou, L.R., Pan, X.H., Tian, Z.J., Xiao, K.Y. and Zhang, Z.W. (2006) Hydrocarbon Formation and Distribution of Rift Basins in Sudan—A Comparative Analysis of Them with Rift Basins in East China. *Petroleum Exploration and Development*, **33**, 255-261.

[41] Macgregor, D.S. (1995) Hydrocarbon Habitat and Classification of Inverted Rift Basins. *Geological Society Special Publication*, **88**, 83-93. https://doi.org/10.1144/GSL.SP.1995.088.01.06

[42] Chen, L., Ji, H., Dou, L., Du, Y., Xu, Z., Zhang, L., Yang, X. and Fu, S. (2018) The Characteristics of Source Rock and Hydrocarbon Charging Time of Precambrian Granite Reservoirs in the Bongor Basin, Chad. *Marine and Petroleum Geology*, **97**, 323-338. https://doi.org/10.1016/j.marpetgeo.2018.06.003

[43] Morris, A. Ferrill, D.A. and Henderson, D.B. (1996) Slip-Tendency Analysis and Fault Reactivation. *Geology*, **24**, 275-278.

https://doi.org/10.1130/0091-7613(1996)024<0275:STAAFR>2.3.CO;2

[44] Streit, J.E. and Hillis, R.R. (2004) Estimating Fault Stability and Sustainable Fluid Pressures for Underground Storage of CO_2 in Porous Rock. *Energy*, **29**, 1445-1456. https://doi.org/10.1016/j.energy.2004.03.078

[45] Lisle, R.J. and Srivastava, D.C. (2004) Test of the Frictional Reactivation Theory for Faults and Validity of Fault-Slip Analysis. *Geology*, **32**, 569-572. https://doi.org/10.1130/G20408.1

[46] Collettini, C. and Trippetta, F. (2007) A Slip Tendency Analysis to Test Mechanical and Structural Control on Aftershock Rupture Planes. *Earth and Planetary Science Letters*, **255**, 402-413. https://doi.org/10.1016/j.epsl.2007.01.001

[47] Barton, C.A., Zoback, M.D. and Moos, D. (1995) Fluid Flow along Potentially Active Faults in Crystalline Rock. *Geology*, **23**, 683-686. https://doi.org/10.1130/0091-7613(1995)023<0683:FFAPAF>2.3.CO;2

[48] Sibson, R.H. (2000) Fluid Involvement in Normal Faulting. *Journal of Geodynamics*, **29**, 469-499. https://doi.org/10.1016/S0264-3707(99)00042-3

[49] Stock, J.M., Healy, J.H., Hickman, S.H. and Zoback, M.D. (1985) Hydraulic Fracturing Stress Measurements at Yucca Mountain, Nevada, and Relationship to the Regional Stress Field (USA). *Journal of Geophysical Research*, **90**, 8691-8706. https://doi.org/10.1029/JB090iB10p08691

[50] Wiprut, D. and Zoback, M.D. (2002) Fault Reactivation, Leakage Potential, and Hydrocarbon Column Heights in the Northern North Sea. *Norweigian Petroleum Society Special Publications*, **11**, 203-219. https://doi.org/10.1016/S0928-8937(02)80016-9

[51] Zhang, X., Koutsabeloulis, N. and Heffer, K. (2007) Hydromechanical Modeling of Critically Stressed and Faulted Reservoirs. *AAPG Bulletin*, **91**, 31-50. https://doi.org/10.1306/08030605136

[52] Zoback, M., Barton, C., Finkbeiner, T. and Dholakia, S. (1996) Evidence for Fluid Flow along Critically-Stressed Faults in Crystalline and Sedimentary Rock. In: Jones, G., Fisher, Q. and Knipe, R., Eds., *Faulting, Faults Sealing and Fluid Flow in Hydrocarbon Reservoirs*, University of Leeds, London, 47-48.

[53] Takatoshi, I. and Kazuo, H. (2003) Role of Stress-Controlled Flow Pathways in HDR Geothermal Reservoirs. *Pure and Applied Geophysics*, **60**, 1103-1124. https://doi.org/10.1007/978-3-0348-8083-1_19

[54] McFarland, J.M., Morris, A.P. and Ferrill, D.A. (2012) Stress Inversion Using Slip Tendency. *Computers and Geosciences*, **41**, 40-46. https://doi.org/10.1016/j.cageo.2011.08.004

[55] Ping, G., Liu, X., Li, M., Zhang, X., Gao, Y., Wang, S. and Liu, X. (2022) Using Seismic Data and Slip Tendency to Estimate Paleostress: A Case Study from Xicaogu Area of Bohai Bay Basin, China. *Frontiers in Earth Science*, **10**, Article ID: 812874. https://doi.org/10.3389/feart.2022.812874

Appendix

Table S1. Details of faults data collection points from basement. n = 1123 fault data points was selected to measure the strike, dip, horizontal slip, vertical fault throw and displacement. For location, see the **Figure 4**.

Fault No	Fault data points	Strike°	Dip°	Horizontal Slip (m)	Vertical Fault Thrown (m)	Displacement (m)
1	1.1	155.07	9.17	378.47	61.13	383.3750354
1	1.2	160.31	7.43	436.57	56.9	440.2623932
1	1.3	174.89	20.7	509.12	192.39	544.2582902
1	1.4	197.78	21.24	550.81	214.13	590.968115
1	1.5	197.95	21.74	590.72	235.61	635.9734196
1	1.6	194.29	35.46	579	412.34	710.8201429
1	1.7	202.16	35.21	523.61	369.46	640.8339283
1	1.8	190.15	38.06	552.8	432.76	702.0463358
1	1.9	199.99	33.56	898.78	596.15	1078.517645
1	1.10	197.09	48.06	569.38	633.69	851.9134936
1	1.11	183.03	47.1	527.05	567.23	774.2942434
1	1.12	190.02	54.52	560.96	786.91	966.3868116
1	1.13	187.81	50.12	571.4	683.86	891.1579319
1	1.14	183.03	34.2	560.16	380.75	677.3107028
1	1.15	195.81	35.94	505.33	366.38	624.1736243
3	3.1	222.31	76.09	47.4	191.37	197.1528263
3	3.2	231.65	81.77	56.63	391.72	395.7922628
4	4.1	68.71	43.14	649.35	608.42	889.8484809
4	4.2	65.82	64.85	299.6	638.23	705.0515534
4	4.3	44.86	53.75	691.45	943.04	1169.370576
4	4.4	38.35	60.2	651.9	1138.09	1311.572513
4	4.5	46.47	58.6	723.86	1192.99	1395.420524
4	4.6	19	73.59	324.22	1101.11	1147.850966
4	4.7	323.05	82.09	121.45	874.57	882.9625062
4	4.8	316.39	81.81	115.51	802.29	810.5626467
4	4.9	366	75.29	270.24	1029.16	1064.048854
5	5.1	203.16	82.33	38.91	288.86	291.4688452
5	5.2	182.57	83.09	40.46	333.98	336.4218364
5	5.3	156.33	82.8	42.39	335.34	338.0086207
6	6.1	216.76	24.9	73.1	33.93	80.59066261
6	6.2	184.58	23.27	67.91	29.2	73.92163486
7	7.1	350.29	72.85	82.18	266.3	278.6920207
7	7.2	40.31	74.12	103.46	363.63	378.0618316

Continued

7	7.3	36.4	13.06	84.64	19.63	86.88651506
7	7.4	50.43	20.74	73.36	27.78	78.44372505
7	7.5	53.16	15.08	134.62	36.27	139.4204336
7	7.6	49.95	17.72	105.19	33.61	110.4290188
7	7.7	22.46	38.77	68.19	54.76	87.45589574
8	8.1	7.98	50.13	229.06	274.2	357.2871725
8	8.2	345.3	6.18	182.63	19.78	183.6980275
8	8.3	12.71	25.11	314.87	147.56	347.7313194
8	8.4	66.07	54.02	117.16	161.37	199.4160036
8	8.5	39.61	67.87	89.04	218.93	236.343958
8	8.6	350.78	46.56	147.67	155.93	214.7570576
10	10.1	198.26	70.55	66.13	187.27	198.6031969
11	11.1	339.86	65.6	27.09	59.72	65.57702723
11	11.2	359.06	67.75	130.27	318.48	344.0926958
11	11.3	19.72	37.87	119.85	93.18	151.8108524
11	11.4	80.48	59.52	114.64	194.76	225.9951044
11	11.5	22.79	71.03	97.02	282.2	298.4119977
11	11.6	7.18	76.63	88.26	371.33	381.674988
12	12.1	195.74	86.08	61.78	902.26	904.3726422
12	12.2	193.32	82.83	67.39	535.32	539.5450996
12	12.3	183.77	84.42	56.27	576.06	578.8017247
12	12.4	170.6	81.1	87.66	559.96	566.7799195
13	13.1	339.37	79.16	39.03	203.84	207.5429751
13	13.2	13.57	78.94	116.44	595.93	607.1991753
13	13.3	343.09	78.76	150.67	758.49	773.3101118
13	13.4	14.05	64.07	294.37	605.35	673.128754
14	14.1	231.77	81.22	33.74	218.34	220.9315351
14	14.2	222.24	83.39	34.47	297.47	299.4604845
15	15.1	8.6	3.71	49.19	3.19	49.29332815
15	15.2	9.24	12.65	69.85	15.68	71.58830142
15	15.3	352.15	52.49	84.91	110.61	139.4427488
15	15.4	15.09	16.88	57.39	17.41	59.97266211
15	15.5	16.54	29.95	189.56	109.23	218.778853
15	15.6	358.23	26.14	277.59	136.21	309.2076522
15	15.7	44.49	52	138.52	177.29	224.9878541
17	17.1	232.34	61.74	32.27	60.02	68.14509007
18	18.1	7.91	68.27	44.86	112.54	121.1514391
18	18.2	17.72	67.45	60.36	145.35	157.3847264

Continued

18	18.3	8.13	65.75	57.73	128.17	140.5713406
18	18.4	3.7	23.99	111.94	49.81	122.5218336
18	18.5	353.66	33.73	169.93	113.45	204.321089
18	18.6	10.5	48.62	272.04	308.83	411.5601177
18	18.7	2.85	39.4	198.16	162.77	256.4399706
19	19.1	201.98	30.25	57.78	33.69	66.884561
19	19.2	183.82	73.98	49.98	174.12	181.1512484
19	19.3	139.74	85.36	49.92	615.09	617.1124002
20	20.1	343.04	51.33	259.78	324.65	415.7923411
20	20.2	332.68	62.13	148.71	281.25	318.1449773
20	20.3	350.06	60.68	453.64	807.74	926.408742
20	20.4	323.04	50.71	445.59	544.59	703.6538326
20	20.5	357.63	9.82	399.99	69.25	405.9403436
20	20.6	18.81	7.47	356.55	46.74	359.6005146
21	21.1	187.02	47.92	901.71	998.55	1345.430424
21	21.2	226.8	54.69	1191.49	1682.12	2061.352982
21	21.3	225.86	55	1154.23	1648.69	2012.56692
21	21.4	232.57	53.38	1218.33	1639.02	2042.232736
21	21.5	208.97	44.38	1572.29	1538.52	2199.804454
21	21.6	199.8	33.52	2245.05	1486.87	2692.774016
21	21.7	246.68	37.77	2224.05	1723.24	2813.530611
21	21.8	242.7	44.58	1757.66	1732.16	2467.741263
21	21.9	218.3	40.23	1467.91	1241.86	1922.752201
21	21.10	186.87	45.47	1137.96	1156.73	1622.645141
21	21.11	183.87	38.42	1273.98	1010.62	1626.154305
21	21.12	205.85	38.16	1679.92	1320.29	2136.655539
21	21.13	195.01	36.07	1732.59	1261.86	2143.398882
21	21.14	195.79	31.41	1817.97	1109.92	2130.008762
21	21.15	185.78	23	1869.05	793.38	2030.467859
21	21.16	193.26	25.97	2043.47	995.43	2273.026732
21	21.17	210.78	28.87	1879.75	1036.21	2146.436868
21	21.18	201.66	33.21	1411.62	923.94	1687.108813
22	22.1	354.91	7.85	50.61	6.98	51.08906439
22	22.2	29.29	8.64	65.34	9.93	66.09024512
23	23.1	228.83	49.74	49.88	58.9	77.18305773
23	23.2	214.14	39.83	50.38	42.01	65.59713789
23	23.3	190.78	52.93	106.11	140.47	176.043043
23	23.4	200.62	72.79	81.68	263.75	276.1081036

Continued

24	24.1	254.95	78.31	105.01	507.51	518.26007
24	24.2	229.35	82.45	78.98	595.82	601.0318734
24	24.3	192.93	83.69	87.04	786.78	791.5798949
24	24.4	194.24	80.22	56.41	327.41	332.233948
24	24.5	203.81	81.82	42.83	297.83	300.8938647
25	25.1	243.84	82.09	40.54	291.83	294.632382
25	25.2	167.89	78.17	66.01	315.21	322.0476117
25	25.3	188.12	73.77	115.23	395.99	412.4148797
25	25.4	200.27	71.24	106.49	313.54	331.1305659
26	26.1	21.32	13.56	138.89	33.51	142.875303
26	26.2	60.21	17.91	133.31	43.07	140.0949
26	26.3	45.63	30	111.62	64.44	128.8857556
26	26.4	28.4	4.26	97.95	7.3	98.22164985
26	26.5	29.76	18.7	89.1	30.15	94.06291777
27	27.1	357.95	21.83	237.57	95.15	255.9160554
27	27.2	354.39	11.37	283.28	56.98	288.9537659
27	27.3	53.72	25.98	392.46	191.24	436.574838
27	27.4	47.02	29.45	540.13	305.02	620.3044553
27	27.5	26.87	29.36	580.48	326.57	666.0367822
27	27.6	40.87	16.79	673.71	203.23	703.6956707
27	27.7	29.85	31.73	377.54	233.48	443.902424
27	27.8	340.07	41.26	593.37	520.6	789.3746366
27	27.9	32.55	24.84	1043.74	483.16	1150.146414
27	27.10	33.91	13.78	1141.36	279.92	1175.18418
27	27.11	23.14	22.85	1029.26	433.63	1116.875608
27	27.12	19.08	32.96	993.97	644.6	1184.687942
27	27.13	20.79	27.93	987.99	523.67	1118.192519
27	27.14	30.6	25.47	958.62	456.61	1061.812129
27	27.15	33.78	10.96	785.7	152.11	800.2886617
27	27.16	11.47	19.71	770.83	276.21	818.8228459
27	27.17	345.88	42.91	550.32	511.52	751.3353531
27	27.18	10.25	55.74	374.1	549.21	664.5166921
27	27.19	10.25	67.67	206.95	503.96	544.7971954
28	28.1	32.64	64.67	306.15	646.72	715.5239904
28	28.2	57.01	62.3	312.66	595.46	672.5540032
28	28.3	37.46	56.52	400.62	605.8	726.2850848
28	28.4	16.25	65.39	541.28	1181.91	1299.959725
28	28.5	66.43	62.83	1011.46	1970.67	2215.082748

Continued

28	28.6	331.22	19.25	1065.22	371.9	1128.274461
29	29.1	177.13	40.98	531.92	462.07	704.5903571
29	29.2	158.06	28.88	488.29	269.31	557.6333923
29	29.3	188.2	45.06	603.19	604.41	853.9025847
29	29.4	203.29	54.4	541.05	755.64	929.3690936
29	29.5	193.16	51.89	792.86	1010.67	1284.55472
29	29.6	229.54	58.58	797.16	1305.15	1529.339919
29	29.7	217.83	67.53	503.04	1216.52	1316.423242
29	29.8	220.99	67.38	398.51	956.26	1035.974617
29	29.9	239.08	53.61	362.82	492.34	611.5856669
29	29.10	229.82	56.72	347.79	529.85	633.7972125
29	29.11	205.72	62.91	338.31	661.54	743.0268015
29	29.12	202.48	59.58	378.74	645.07	748.0369593
29	29.13	201	55.46	361.21	524.73	637.0355069
29	29.14	205.49	51.55	350.62	441.61	563.8739012
29	29.15	173.25	48.32	294.02	330.18	442.11604
31	31.1	337.96	14.24	618.1	156.86	637.693241
31	31.2	347.89	14.46	1184.69	305.47	1223.438726
31	31.3	349.47	12.44	1531.79	337.94	1568.624891
31	31.4	7.27	17.05	1678.55	514.69	1755.686731
31	31.5	359.45	20.05	1825.19	666.21	1942.97563
31	31.6	343.85	21.86	1629.02	653.52	1755.219232
31	31.7	365.59	22.35	1272.41	523.09	1375.736296
31	31.8	356.03	33.49	928.62	614.47	1113.51178
31	31.9	343.41	34.21	850.34	578.11	1028.245733
31	31.10	15.75	29.79	1198.49	686.1	1380.982075
31	31.11	14.53	27.82	1233.54	650.8	1394.690493
31	31.12	22.23	22.91	1272.39	537.71	1381.342954
31	31.13	31.95	24.62	1116.13	511.54	1227.770072
31	31.14	25.52	28.38	840.07	453.88	954.8427406
31	31.15	16.31	7.28	601.23	76.77	606.1114962
32	32.1	150.35	60.97	166.53	300.01	343.1300643
32	32.2	145.66	63.02	161.3	316.83	355.5262844
32	32.3	150.5	71.98	137.79	423.6	445.447016
32	32.4	152.7	40.81	192.72	166.44	254.6434213
32	32.5	171.53	72.04	197.7	609.87	641.1136459
32	32.6	157.88	59.68	174.91	299.09	346.4799218
32	32.7	143.2	45.68	124.61	127.59	178.344779

Continued

33	33.1	191	51.83	287.66	365.97	465.4914784
33	33.2	200.59	67.59	333.15	807.86	873.8573694
33	33.3	219.27	69.08	292.61	765.54	819.5560406
33	33.4	220.69	68.87	284.88	737.25	790.3759719
33	33.5	201.49	67.85	354.42	870.74	940.1072726
33	33.6	209.98	66.24	384.38	872.99	953.8655694
33	33.7	209.61	32.51	282.53	180.09	335.045682
33	33.8	203.89	69.1	359.47	941.57	1007.855518
33	33.9	231.68	73.99	290.56	1012.52	1053.385905
33	33.10	220.76	76.04	279.62	1124.59	1158.831313
33	33.11	239.12	74.27	284.12	1008.56	1047.81556
33	33.12	209.34	71.55	473.81	1420.07	1497.028631
33	33.13	185.81	66.85	646.04	1511.2	1643.500265
33	33.14	190.11	62.65	775.93	1499.93	1688.744317
33	33.15	200.44	55.89	1050.89	1551.35	1873.781368
33	33.16	189.32	65.45	678.01	1484.34	1631.858694
34	34.1	190.78	17.44	179.84	56.5	188.5064338
34	34.2	194.84	40.38	185.11	157.46	243.0213236
34	34.3	212.88	34.82	206.98	143.97	252.1271134
34	34.4	158.97	31.92	213.02	132.71	250.9770199
34	34.5	158.33	28.68	886.14	484.79	1010.0819
34	34.6	218.05	27.03	1057.33	539.45	1186.993274
35	35.1	163.74	72.23	134.81	420.56	441.6383698
35	35.2	184.45	71.64	141.39	426.03	448.8793747
35	35.3	173.82	69.2	199.02	523.87	560.4005151
35	35.4	170.32	76.56	85.8	359.03	369.139785
35	35.5	191.72	69.62	108.39	291.77	311.25251
35	35.6	214.35	61.43	109.47	201.01	228.8857816
35	35.7	206.53	75.06	105.13	393.9	407.6880264
35	35.8	195.54	70.13	108.16	299.3	318.2437362
36	36.1	35.3	21.84	238.08	95.42	256.4898883
36	36.2	13.61	38.95	249.67	201.8	321.0270221
36	36.3	12.72	19.58	260.35	92.59	276.3241405
36	36.4	352.7	33.84	257.36	172.57	309.8621863
36	36.5	41.18	35.46	382.98	272.8	470.2058277
36	36.6	25.07	39.31	300.66	246.19	388.5948426
36	36.7	4.56	41.47	288.43	254.95	384.9563188
36	36.8	16.43	38.03	244.43	191.17	310.3095129

Continued

36	36.9	15.29	37.53	205.59	157.93	259.247243
36	36.10	357.57	49.11	205.91	237.81	314.5672014
36	36.11	357.57	42.92	335.99	312.45	458.8183547
36	36.12	25.94	33.04	382.36	248.7	456.1259252
36	36.13	4.52	36.97	428.91	322.9	536.8688835
36	36.14	343.89	27.88	402.43	212.92	455.2854394
37	37.1	145.16	23.37	959.42	414.55	1045.14996
37	37.2	147.81	39.1	1330.77	1081.65	1714.909769
37	37.3	149.67	47.62	1248.49	1368.3	1852.28836
37	37.4	149.68	46.7	1208.25	1282.16	1761.761144
37	37.5	139.64	46.79	1252.86	1333.82	1829.954637
37	37.6	140.11	49.93	1365.64	1623.4	2121.414662
37	37.7	139.11	49.74	1501.09	1772.72	2322.887726
37	37.8	135.12	47.92	1556.17	1723.56	2322.137839
37	37.9	136.1	49.5	1498.83	1754.85	2307.810627
37	37.10	136.94	47.23	1552.53	1678.59	2286.485029
37	37.11	153.6	51.45	1476.24	1852.64	2368.873046
37	37.12	146.88	49.46	1587.95	1856.83	2443.236143
37	37.13	150.67	45.88	1688.95	1741.7	2426.122625
37	37.14	151.34	35.8	1766.16	1273.99	2177.698709
37	37.15	180.65	25.55	1505.86	719.73	1669.019357
37	37.16	150.46	28.25	1211.33	650.94	1375.152083
37	37.17	140.96	23.98	1209.24	537.78	1323.430658
37	37.18	163.09	27.43	1023.5	531.24	1153.155752
37	37.19	141.64	36.15	900.83	658.19	1115.665167
37	37.20	146.13	40.54	1006.13	860.39	1323.846112
37	37.21	142.47	42.66	1043.96	961.91	1419.550397
37	37.22	152.17	43.62	1075.84	1025.31	1486.166983
37	37.23	157.21	47.46	983.66	1071.97	1454.890606
37	37.24	171.29	44.68	874.67	864.94	1230.109269
37	37.25	150.69	44.65	822.43	812.55	1156.126553
37	37.26	167.42	45.48	867.06	881.74	1236.631906
37	37.27	142.23	45.06	916.65	918.44	1297.6052
37	37.28	140.58	61.99	1018.91	1915.4	2169.54713
37	37.29	135.35	66.9	1009.67	2367.07	2573.412888
37	37.30	139.77	69.22	973.88	2566.86	2745.398425
37	37.31	137.76	67.5	847.82	2046.66	2215.313952
37	37.32	147.86	75.58	652.27	2536.55	2619.072747

Continued

37	37.33	136.65	77.72	598.11	2746.71	2811.076555
37	37.34	136.56	74.7	836.81	3058.87	3171.267358
37	37.35	139.35	70.4	1274.08	3578.82	3798.846198
37	37.36	136.4	58.97	2251.66	3742.42	3367.571432
37-1	37-1.1	186.76	48.85	2999.73	3432.32	3558.420851
37-2	37-1.2	174.06	44.99	3589.12	3587.37	3074.544895
37-3	37-1.3	185.9	42.42	3711.31	3391.67	3027.648288
37-4	37-1.4	180.07	40.67	3849.53	3308.06	3075.642047
37-5	37-1.5	169.81	36.87	4506.26	3379.14	3632.492017
37-6	37-1.6	233.05	37.97	4580.12	3574.02	3809.571256
37-7	37-1.7	229.12	41.28	4008.12	3518.65	3333.472017
37-8	37-1.8	217.7	42.42	4010.55	3664.33	3432.478776
37-9	37-1.9	225.91	46.38	3461.4	3632.33	3017.480562
37-10	37-1.10	225.73	46.6	3201.25	3385.72	3659.517301
37-11	37-1.11	225.36	44.54	3279.66	3227.71	3601.552082
37-12	37-1.12	224.58	46.3	2965.55	3103.03	3292.23508
37-13	37-1.13	211.6	48.61	2638.32	2994.07	3990.637491
37-14	37-1.14	227.17	49.59	2349.72	2759.94	3624.700385
37-15	37-1.15	210.19	48.07	2290.63	2549.96	3427.722538
37-16	37-1.16	223.21	48.38	2136.02	2403.92	3215.806712
37-17	37-1.17	212.8	44.25	2342.15	2281.23	3269.50714
37-18	37-1.18	195.44	37.79	2741.55	2125.76	3469.142831
37-19	37-1.19	192.86	29.56	3705.96	2102.01	3260.58512
37-20	37-1.20	191.52	23.66	4748.6	2080.8	3184.489425
37-21	37-1.21	184.7	23.16	5479.97	2344.53	3960.443953
37-22	37-1.22	183.23	22.88	5885.47	2483.41	3387.963866
37-23	37-1.23	183.12	13.21	4705.84	1104.95	3833.822981
37-24	37-1.24	183.23	14.6	3770.5	982.07	3896.297183
37-25	37-1.25	182.84	16.36	2781.89	816.44	2899.221662
37-26	37-1.26	183.46	9.41	1816.96	300.98	1841.720012
37-27	37-1.27	195.3	13.28	1258.58	297.05	1293.15982
37-28	37-1.28	217.62	32.72	925.85	594.74	1100.415326
37-29	37-1.29	223.71	40.32	659.21	559.38	864.559893
37-30	37-1.30	182.71	49.27	274.47	318.7	420.5989431
37-31	37-1.31	189.06	55.22	263.22	379.06	461.4880844
37-32	37-1.32	188.36	61.13	196.06	355.54	406.0150431
38	38.1	29.62	3.15	336.02	18.51	336.5294348
38	38.2	41.9	5.14	561.74	50.49	564.0044926

Continued

38	38.3	57.02	8.52	894.45	133.96	904.4258312
38	38.4	76.3	15.1	1052.32	283.95	1089.956414
38	38.5	57.37	5.65	1112.44	110.07	1117.872157
38	38.6	51.08	11.76	1227.95	255.64	1254.277885
38	38.7	45.1	9.8	1381.57	238.76	1402.049215
38	38.8	42.65	13.16	1392.07	325.4	1429.595763
38	38.9	43.46	19.67	1286.25	459.71	1365.932775
38	38.10	29.83	20.13	1289.04	472.41	1372.878483
38	38.11	29.61	14.21	1325.59	335.69	1367.434322
38	38.12	28.92	8.37	1353.13	198.97	1367.680466
38	38.13	37.24	3.66	1361.62	87.13	1364.404874
38	38.14	38.97	6.6	1383.06	160.13	1392.299027
38	38.15	29.34	4.33	1437.29	108.94	1441.412664
38	38.16	36.31	2.42	1360.39	57.41	1361.600845
38	38.17	30.09	3.66	1319.06	84.4	1321.757407
38	38.18	29.28	6.69	1331.88	156.11	1340.997639
38	38.19	32.77	14.49	1182.85	305.58	1221.684599
38	38.20	28.22	19.49	1058.42	374.53	1122.73132
38	38.21	26.19	23.81	941.17	415.27	1028.712857
38	38.22	24.76	22.85	954.96	402.35	1036.25968
38	38.23	23.9	21.1	912.55	352.12	978.1288243
39	39.1	343.52	16.56	253.8	75.47	264.7832338
39	39.2	341.78	8.22	223.23	32.26	225.5489758
39	39.3	334.04	5.41	222.66	21.08	223.6556326
39	39.4	333.82	6.31	218.13	24.1	219.4573009
39	39.5	8.5	22.39	387.88	159.8	419.507967
39	39.6	28.24	29.42	378.97	213.75	435.0946143
39	39.7	14.83	11.68	344.06	71.13	351.3356807
39	39.8	318.78	37.71	371.04	286.87	469.0043481
39	39.9	348.48	32.89	461	298.15	549.0122244
39	39.10	12.54	36.91	375.29	281.87	469.3541105
40	40.1	346.47	7.09	342.4	42.6	345.0398818
40	40.2	347.81	9.87	321.42	55.91	326.2464475
40	40.3	342.66	31.26	327.05	198.52	382.5857981
40	40.4	20.98	29.62	526.19	299.18	605.2971076
40	40.5	330.41	35.28	490.79	347.29	601.2363663
40	40.6	359.27	41.52	311.67	275.98	416.2969485
40	40.7	25.98	50.77	271.66	332.71	429.5289277

Continued

40	40.8	359.12	10.03	282.54	49.97	286.9248203
40	40.9	3.94	38.12	306.91	240.85	390.1313504
40	40.10	327.9	44.33	396.61	387.38	554.4030632
40	40.11	321	53.15	432.23	576.69	720.6900367
40	40.12	356.83	38.22	705.94	555.91	898.5472785
40	40.13	356.9	33.9	777.97	522.75	937.2859134
41	41.1	1.7	37.53	242.05	185.96	305.2365052
41	41.2	12.4	16.17	284.88	82.62	296.6187432
41	41.3	42.84	38.15	304.19	238.97	386.8309928
41	41.4	55.93	44.81	360.98	358.53	508.7733496
41	41.5	57.26	58.49	329.32	537.12	630.0393296
41	41.6	71.56	59.08	364.07	607.77	708.471127
41	41.7	71.5	49.6	448.05	526.41	691.2715028
41	41.8	32.86	4.81	962.7	80.96	966.0982412
41	41.9	30.55	15.52	751.99	208.79	780.4372007
41	41.10	349.79	57.35	495.18	772.95	917.9623821
41	41.11	335.85	37.65	924.09	712.9	1167.119847
41	41.12	14.52	33.24	1092.56	715.97	1306.254338
41	41.13	72.2	39.69	878.43	729.09	1141.582889
41	41.14	78.02	33.27	607.51	398.6	726.6019268
41	41.15	24.97	32.7	777.82	499.44	924.3615451
41	41.16	357.79	33.58	734.3	487.58	881.4367512
41	41.17	354.9	39.84	582.71	486.12	758.8567707
41	41.18	341.16	34.43	547.74	375.48	664.0815748
41	41.19	348.56	30.42	711.13	417.47	824.6132899
41	41.20	17.65	38.31	711.62	562.16	906.8775496
41	41.21	17.95	39.04	603.39	489.28	776.8361542
41	41.22	34.86	15.98	332.35	95.15	345.7022491
41	41.23	34.49	16.44	346.01	102.1	360.7593798
41	41.24	9.54	30.33	344.56	201.62	399.2145012
42	42.1	131.56	34.53	227.4	156.47	276.0319201
42	42.2	134.79	31.47	274.88	168.26	322.2893762
42	42.3	95.41	24.25	415.06	187	455.24038
42	42.4	126.55	31.93	540.12	336.61	636.4243133
42	42.5	129.1	23.07	486.22	207.08	528.4808557
43	43.1	43.54	12.24	231.95	50.3	237.3412996
43	43.2	351.65	10.25	257.98	46.66	262.1656652
43	43.3	4.95	19.34	436.13	153.05	462.2052351

Continued

43	43.4	7.09	24.35	627.42	283.93	688.6741619
43	43.5	16.71	30.68	520.23	308.7	604.9255681
43	43.6	28.24	10.45	265.19	48.9	269.6607982
43	43.7	23.26	0.3	309.2	1.64	309.2043493
43	43.8	8.9	14.3	156.83	39.97	161.8432878
44	44.1	59.23	43.03	604.39	564.1	826.7382186
44	44.2	44.29	40.95	605.95	525.83	802.2920861
44	44.3	4.08	43.96	698.4	673.46	970.2117973
44	44.4	11.43	38.52	903.64	719.26	1154.945972
44	44.5	16.48	15.29	589.43	161.16	611.064866
44	44.6	39.67	28.28	431.82	232.36	490.3668851
44	44.7	22.64	10.22	366.87	66.16	372.7877982
44	44.8	25.89	15.07	372.49	100.26	385.7471551
44	44.9	29.31	16.18	439.89	127.67	458.0424009
44	44.10	28.84	9.44	440.92	73.32	446.9745729
44	44.11	68.36	3.05	443.78	23.63	444.4086692
44	44.12	15.33	4.67	390.42	31.87	391.718615
44	44.13	43.94	13	494.68	114.18	507.6862957
44	44.14	36.39	43.09	281.09	262.97	384.9218219
44	44.15	20.06	15.67	411.66	115.48	427.5506824
44	44.16	7.46	6.44	557.13	62.91	560.6705851
44	44.17	6.61	19.29	421.75	147.62	446.8385916
44	44.18	21.26	19.53	438.15	155.38	464.8853266
44	44.19	32.41	15.33	316.16	86.66	327.8217522
44	44.20	18.52	10.8	291.75	55.64	297.0082021
44	44.21	16.97	0.99	290.17	5	290.213075
45	45.1	342.81	8.67	153.37	23.4	155.1448256
45	45.2	2.78	44.16	185.25	179.9	258.2277532
45	45.3	17.62	54.2	159.47	221.13	272.633743
46	46.1	39.87	6.77	271.16	32.19	273.0639883
46	46.2	346.85	13.16	373.1	87.26	383.1682628
46	46.3	20.72	2.21	566.54	21.89	566.9627357
46	46.4	354.29	18.78	483.12	164.24	510.2741538
46	46.5	355.7	25.25	536.62	253.03	593.2834106
46	46.6	35.45	22.25	805.21	329.46	870.0040435
46	46.7	46.18	21.04	855.39	328.99	916.4750254
46	46.8	31.58	21.5	962.49	379.23	1034.505869
46	46.9	15.45	34.54	684.38	471.06	830.8270024

Continued

47	47.1	347.69	45.66	607.28	621.43	868.8867839
47	47.2	320.23	60.17	582.3	1015.35	1170.473798
47	47.3	302.23	40.08	1472.32	1238.84	1924.175337
47	47.4	44.37	23	1553.79	659.57	1687.985767
47	47.5	24.23	19.65	1690.64	603.75	1795.209646
47	47.6	19.62	17.4	1748.53	547.86	1832.350332
47	47.7	11.8	17.75	1673.74	535.81	1757.412286
47	47.8	359.1	23.42	1781.58	771.82	1941.580132
47	47.9	334.25	26.57	1393.02	696.53	1557.452651
47	47.10	318.64	34.03	1190.26	803.7	1436.193774
47	47.11	58.01	24	923.17	411.02	1010.534655
47	47.12	38.89	37.55	443.86	341.2	559.8474253
47	47.13	352.93	35.36	722.69	512.74	886.1056053
47	47.14	32.84	49.13	870.91	1006.32	1330.85092
47	47.15	64.02	45.84	561.03	577.77	805.3401976
47	47.16	19.49	20.93	479.27	183.34	513.1406128
47	47.17	332.09	6.97	835.99	102.14	842.2065422
47	47.18	338.89	6.22	1826.49	199.08	1837.307423
47	47.19	74.54	8.2	2620.57	377.75	2647.65598
47	47.20	15.95	39.35	2282.23	1871.2	2951.26468
47	47.21	351.03	43.17	1954.9	1834	2680.520474
47	47.22	29.98	45.21	2091.33	2106.59	2968.397311
47	47.23	1.62	45.93	2000	2066.31	2875.697657
47	47.24	1.26	38.88	2161.6	1742.91	2776.733662
47	47.25	43.27	30.54	2642.29	1558.74	3067.795109
47	47.26	55.12	30.1	2928.12	1697.25	3384.456278
47	47.27	55.17	29.47	2437.66	1377.32	2799.856542
47	47.28	43.4	27.86	2111.49	1116.23	2388.380086
47	47.29	43.5	30.81	1493.22	890.44	1738.559565
47	47.30	43.74	55.46	903.63	1312.83	1593.759639
47	47.31	55.51	59.9	736.03	1269.94	1467.817347
47	47.32	56.45	56.9	639.05	980.34	1170.235625
47	47.33	47.65	54.26	457.01	635.05	782.3980078
47	47.34	345.24	12.02	439.49	93.54	449.3341648
47	47.35	350.94	6.27	492.91	54.17	495.8776633
47	47.36	27.65	13.73	415.45	101.51	427.6715826
47	47.37	51.27	21.17	338	130.91	362.4657613
48	48.4	326.73	51.59	166.39	209.85	267.810856

Continued

48	48.5	2.19	5.62	155.22	15.27	155.969296
48	48.6	35.98	52.33	148.99	193.01	243.8255118
48	48.7	9.82	32.94	103.99	67.37	123.9057585
48	48.8	1.3	30.98	135.1	81.1	157.5729038
48	48.9	1.03	32.67	80.46	51.6	95.58436902
48	48.10	3.27	46.61	104.44	110.46	152.0168583
48	48.11	22.45	19.18	98.31	34.2	104.0888856
49	49.1	219.18	61.78	216.09	402.64	456.9615495
49	49.2	229.98	53.93	585.52	803.9	994.5294769
49	49.3	235.71	57.76	553.17	877.11	1036.975892
49	49.4	239.48	62.1	479.85	906.13	1025.342674
49	49.5	227.95	69.5	415.59	1111.54	1186.691291
49	49.6	218.96	71.12	512.91	1499.69	1584.97532
49	49.7	260.8	65.75	756.15	1678.65	1841.094415
49	49.8	228.74	72.44	576.72	1822.28	1911.363481
49	49.9	232.46	71.03	526.2	1531.08	1618.978816
49	49.10	241.33	42.91	735.33	683.6	1004.001578
49	49.11	216.53	64.88	571.05	1217.81	1345.049924
49	49.12	207.61	61.73	482.87	897.97	1019.565377
49	49.13	197.82	49.4	330.29	385.38	507.5521929
49	49.14	206.3	44.65	241.78	238.86	339.8700752
49	49.15	225.22	44.27	157.02	153.09	219.2984918
49	49.16	219.48	31.95	99.06	61.79	116.7513927
49	49.17	233.08	20.98	141.54	54.27	151.5876133
50	50.1	196.99	52.1	123.84	159.06	201.5847941
50	50.2	229.83	64.61	161.68	340.62	377.0443035
50	50.3	237.68	51.48	198.4	249.26	318.5798292
50	50.4	205.91	62.23	363.56	690.45	780.3185735
50	50.5	194.36	66.46	426.98	980.08	1069.050386
50	50.6	189.63	71.79	247.88	753.33	793.0640474
51	51.1	186.15	68.04	247.13	613.04	660.9775174
51	51.2	164.33	35.77	578.32	416.57	712.7303749
51	51.3	145.97	37.99	744.37	581.39	944.5109999
51	51.4	153.9	44.34	991.06	968.59	1385.772893
51	51.5	163.98	21.11	952.68	367.78	1021.205812
52	52.1	6.08	10.89	551.23	106.08	561.34435
52	52.2	356.71	6.06	459.96	48.83	462.5446687
52	52.3	353.31	23.96	385.73	171.44	422.1129073

Continued

52	52.4	350.13	7.42	236.84	30.84	238.8394674
52	52.5	343.63	29.59	281.88	160.06	324.1535716
52	52.6	10.8	23.82	249.65	110.2	272.8903855
52	52.7	14.61	29.7	173.45	98.93	199.6798623
52	52.8	13	20.85	239.5	91.22	256.2837069
52	52.9	21.82	4.88	182.8	15.61	183.4652885
52	52.10	38.92	16.46	181.2	53.55	188.947195
52	52.11	24.89	44.35	221.18	216.24	309.3223723
52	52.12	30.78	59.05	175.91	293.37	342.0676614
52	52.13	24.43	57.51	134.45	211.14	250.3136075
52	52.14	79.2	36.2	113.2	82.85	140.2795869
53	53.1	25.48	6.21	194.86	21.19	196.0087643
53	53.2	23.03	5.32	129.56	12.05	130.1191612
53	53.3	8.27	5.05	151.97	13.42	152.5613886
53	53.4	43.54	35.59	114.32	81.8	140.5713427
53	53.5	25.32	29.07	107.94	60.01	123.4999745
53	53.6	21.46	41.74	115.81	103.32	155.1998019
54	54.1	185.63	2.52	178.19	7.84	178.3623887
54	54.2	182.49	1.58	353.4	9.75	353.5344714
54	54.3	165.86	13.19	390.1	91.46	400.6781022
54	54.4	179.6	42	652.17	587.22	877.5836355
54	54.5	178.9	46.02	760.27	787.92	1094.910224
54	54.6	169.97	45.52	799.83	814.62	1141.636445
54	54.7	152.18	32.59	1068.56	683.22	1268.309916
54	54.8	204.84	31.61	884.1	544.05	1038.086322
54	54.9	196.07	26.68	707.26	355.43	791.5473407
54	54.10	214.69	15.07	694.18	186.89	718.8975897
54	54.11	233.01	20.8	623.33	236.79	666.7906666
54	54.12	212.33	45.79	662.33	680.73	949.7759535
54	54.13	212.91	59.35	607.52	1025.41	1191.866695
54	54.14	203.16	58.19	684.06	1103.04	1297.935023
54	54.15	199.56	48.94	709.06	814.09	1079.587241
54	54.16	200.44	32.58	721.53	461.02	856.2388576
54	54.17	198.78	30.75	748.97	445.58	871.4915934
54	54.18	199.06	36.3	774.16	568.58	960.5242954
54	54.19	202.03	40.35	734.73	624.26	964.1206981
54	54.20	199.42	43.74	704.06	673.69	974.4530259
54	54.21	194.76	48.16	723.18	807.68	1084.12928

Continued

54	54.22	194.84	51.74	750.05	950.93	1211.132886
54	54.23	198.01	52.9	684.16	904.72	1134.280911
54	54.24	197.7	57.55	662.94	1042.5	1235.433403
54	54.25	217.39	57.84	635.5	1010.86	1194.026042
54	54.26	221.88	46.87	680.15	725.96	994.7974387
54	54.27	204.38	40.73	607.51	523.18	801.7391798
54	54.28	191.62	23.87	599.72	265.4	655.8210414
54	54.29	194.91	5.77	658.73	66.55	662.0831635
54	54.30	198.06	2.37	595.8	24.7	596.3117725
54	54.31	188.71	0.74	579.55	7.44	579.5977537
54	54.32	194.9	2.66	476	22.14	476.5146164
55	55.1	290.12	59.21	249.3	418.36	487.0067552
55	55.2	329.65	53.75	226.53	308.93	383.0843064
55	55.3	319.67	61.04	133.96	242.05	276.6468581
55	55.4	319.25	65.4	112.51	245.7	270.2350645
55	55.5	296.82	80.18	146.61	846.81	859.4077427
56	56.1	228.66	50.27	755.52	909.18	1182.124673
56	56.2	190.87	48.4	694.15	781.83	1045.515362
56	56.3	183.49	53.59	612.65	830.66	1032.15118
56	56.4	144.97	41.77	912.27	814.84	1223.192862
56	56.5	210.48	46.96	1351.88	1447.6	1980.688086
58	58.1	15.16	41.55	266.19	235.92	355.6899809
58	58.2	22.91	13.81	217.4	53.42	223.8670507
59	59.1	51.84	9.96	323.96	56.87	328.9137858
59	59.2	53.05	29.09	404.67	225.16	463.0926846
59	59.3	54.55	32.29	391.31	247.32	462.9154334
59	59.4	36.2	26.69	499.54	251.18	559.1346922
59	59.5	41.18	27.01	528.99	269.68	593.7657135
59	59.6	35.23	21.78	572.66	228.76	616.6608575
59	59.7	46.11	25.53	415.85	198.64	460.856889
59	59.8	15.48	16.57	379.94	113.02	396.3936478
59	59.9	12.16	19.77	315.74	113.5	335.5204876
60	60.1	64.47	10.88	162.72	31.27	165.6973485
60	60.2	57.2	6.66	341.02	39.79	343.3334888
60	60.3	37.78	29.69	360.33	205.42	414.771124
60	60.4	7.26	23.46	543.49	235.85	592.458102
60	60.5	2.4	23.44	945	409.78	1030.021674
60	60.6	7.55	33.21	903.7	591.49	1080.062086

Continued

60	60.7	5.81	36.35	1012.79	745.37	1257.505476
60	60.8	5.36	36.14	1211.03	884.25	1499.497157
60	60.9	10.35	38.41	935.29	741.55	1193.592806
60	60.10	11.57	49.83	620.45	734.98	961.8491581
60	60.11	6.94	50.85	764.92	939.72	1211.683244
60	60.12	5.42	45.78	863.9	887.9	1238.825904
60	60.13	327.53	31.2	1411.5	854.74	1650.125061
60	60.14	315.53	12.77	2308.1	523.02	2366.616896
60	60.15	4.83	28.35	2510.89	1354.54	2852.954119
60	60.16	355.11	33.59	2407.56	1599.25	2890.31931
60	60.17	347.68	32.82	2433.79	1569.8	2896.136358
60	60.18	24.05	35.43	2405.23	1711.01	2951.726033
60	60.19	17.21	36.47	2275.39	1682.16	2829.675232
60	60.20	3.86	47.25	1720.82	1861.64	2535.138056
60	60.21	346.22	47.78	1723.42	1899.53	2564.837367
60	60.22	329.07	33.05	2536.04	1649.85	3025.475814
60	60.23	36.38	27.37	2247.48	1163.3	2530.698173
60	60.24	25.62	21.91	1546.06	621.85	1666.433001
60	60.25	7.79	21.33	1758.46	686.81	1887.826673
60	60.26	9.66	22.87	2430.83	1025.33	2638.225938
60	60.27	39.85	28.44	2679.96	1451.42	3047.754193
60	60.28	39.84	32.57	2497.38	1595.26	2963.403673
60	60.29	31.74	31.96	2685.98	1675.87	3165.916742
60	60.30	30.55	29.69	3121.9	1780.18	3593.786366
60	60.31	21.72	27.38	3136.1	1624.21	3531.739137
60	60.32	35.34	30.79	2958.92	1763.16	3444.40717
60	60.33	58.97	26.27	2702.53	1333.65	3013.683912
60	60.34	52.13	24.72	2119.69	976.05	2333.615071
60	60.35	42.94	26.04	1433.18	700.35	1595.14734
60	60.36	32.61	23.6	1348.21	588.92	1471.222951
60	60.37	20.93	25.18	1559.23	733.13	1722.985139
60	60.38	351.11	38.78	1189.73	955.83	1526.128586
60	60.39	30.16	39.36	1295.04	1062.22	1674.944754
60	60.40	24.71	43.44	1142.81	1082.17	1573.882653
60	60.41	17.61	37.22	1202.57	913.55	1510.214623
61	61.1	336.31	21.61	324.5	128.55	349.0348872
61	61.2	325.58	47	429.34	460.35	629.4878538
61	61.3	12.13	49.11	613.82	708.77	937.6192752

Continued

62	62.1	313.57	74.6	262.94	954.56	990.1122346
62	62.2	306.75	69.36	279.52	741.95	792.856376
62	62.3	303.68	81.02	129.75	820.74	830.932735
63	63.1	3.07	44.33	474.56	463.59	663.4175772
63	63.2	21.76	36.58	510.93	379.12	636.2243624
63	63.3	340.43	52.18	376.43	484.96	613.9102105
63	63.4	339.15	54.74	417.78	590.97	723.7303844
63	63.5	14.76	52.41	770.4	1000.72	1262.915943
63	63.6	58.4	58.31	741.95	1201.93	1412.489125
63	63.7	61.58	36.89	434.52	326.17	543.3180462
63	63.8	56.27	47.31	213.92	231.89	315.4912653
64	64.1	183.09	75.13	106.59	401.41	415.3208593
64	64.2	184.59	73.22	195.58	648.47	677.3218417
64	64.3	186.41	63.46	251.06	502.61	561.8255385
64	64.4	167.75	59.26	284.11	477.8	555.8878773
64	64.5	175.32	65.44	292.98	641.05	704.8279101
64	64.6	175.96	48.56	356.89	404.24	539.2406232
64	64.7	179.35	52.1	455.15	584.69	740.9614825
64	64.8	188.48	72.5	386.11	1224.87	1284.284801
64	64.9	198.74	66.89	384.67	901.59	980.2221876
64	64.10	226.49	47.68	765.09	840.31	1136.434602
64	64.11	226.28	53.43	595.13	802.29	998.9239015
64	64.12	198.68	55.09	471.73	675.88	824.2226443
64	64.13	191.62	56	441.94	655.22	790.3317101
64	64.14	190.89	57.86	390.3	621.25	733.6795298
64	64.15	122.68	28.2	916.05	491.19	1039.430237
64	64.16	205.07	24.7	1078.1	495.78	1186.632807
64	64.17	235.4	38.31	865.67	683.83	1103.180864
64	64.18	233.8	43.2	703.33	660.5	964.8488684
64	64.19	201.69	41.5	817.85	723.53	1091.95892
64	64.20	205.29	43.94	1023.65	986.45	1421.598722
64	64.21	214.83	45.05	1231.23	1233.6	1742.898813
64	64.22	259.02	48.51	712.41	805.6	1075.415905
64	64.23	223.76	55.98	590.35	874.64	1055.229005
64	64.24	204.02	35.29	942.17	666.93	1154.330946
64	64.25	219.58	33.2	992.78	649.74	1186.496606
64	64.26	217.54	38.24	773.25	609.28	984.4479066
64	64.27	228.33	34.05	679.72	459.29	820.3454044

Continued

64	64.28	235.44	38.15	568.3	446.33	722.6170209
65	65.1	348.97	4.15	152.16	11.04	152.559979
65	65.2	353.2	22.99	138.65	58.83	150.6147118
65	65.3	372.26	15.44	234.13	64.66	242.8945708
65	65.4	344.63	14.5	326.6	84.46	337.3441145
65	65.5	332.4	19.42	509.86	179.71	540.6042024
65	65.6	343.49	29.91	529.78	304.78	611.1936655
65	65.7	358.1	21.15	641.73	248.31	688.0953778
65	65.8	356.19	5.16	388.94	35.09	390.5196944
65	65.9	19.08	1.54	234.41	6.31	234.494913
65	65.10	14.43	7.71	171.63	23.23	173.1949474
66	66.1	64.35	2.17	246.97	9.37	247.1476842
66	66.2	38.57	15.69	386.87	108.65	401.8373046
66	66.3	29.82	18.3	356.56	117.93	375.5562787
66	66.4	30.82	13.01	348.48	80.51	357.6592939
66	66.5	27.06	7.3	334.88	42.92	337.6192246
66	66.6	52.95	14.22	256.53	65.02	264.6417225
66	66.7	30.65	2.57	425.49	19.13	425.9198246
66	66.8	358.76	5.96	396.6	41.43	398.7580782
66	66.9	2.36	12.6	373.69	83.53	382.9118397
66	66.10	20.58	1.09	344.44	6.54	344.502083
67	67.1	178.73	71.02	151.55	440.74	466.0677527
67	67.2	194.93	69.14	147.37	386.64	413.7733758
67	67.3	193.6	44.84	303.72	302.03	428.3315997
67	67.4	190.61	59.4	142.07	240.27	279.1300016
68	68.1	161.05	6.63	287.04	33.37	288.9732142
68	68.2	158.17	10	292.2	51.54	296.710653
68	68.3	171	15.45	330.52	91.33	342.9061669
68	68.4	193.9	5	332.36	29.11	333.6323751
68	68.5	196.26	9.81	307.29	53.12	311.8475244
68	68.6	156.77	26.62	250.75	125.68	280.4835555
68	68.7	193.52	32.3	380.26	240.37	449.8615393
68	68.8	197.63	45.15	404.58	406.66	573.6351907
68	68.9	186.51	49.52	327.83	384.15	505.0185456
68	68.10	186.26	51.66	328.96	415.88	530.255463
68	68.11	203.55	55	324.74	463.78	566.169547
68	68.12	216.22	52.39	463.68	601.98	759.8546327
68	68.13	229.57	47.3	667.62	723.56	984.5077643

Continued

68	68.14	225.35	60.19	303.68	530.1	610.9235242
68	68.15	194.73	70.71	214.76	613.65	650.1447378
68	68.16	223.34	67.62	318.66	773.91	836.9473602
68	68.17	201.67	68.53	283.03	719.55	773.2128966
68	68.18	210.27	35.3	280.31	198.43	343.4358179
68	68.19	234.43	36.61	236.59	175.8	294.7549289
71	71.1	183.5	7.84	254.52	35.06	256.923401
71	71.2	181.33	0.51	287.4	2.58	287.4115801
71	71.3	184.57	13.55	236.38	56.97	243.1482784
71	71.4	199.61	38.37	263.67	208.73	336.2886882
71	71.5	191.71	42.35	262.35	239.14	354.9865661
71	71.6	210.81	25.39	273.18	129.67	302.3931568
71	71.7	201.07	36.73	293.38	218.91	366.0511064
71	71.8	188.51	23.89	329.91	146.11	360.8167682
71	71.9	245.39	41.05	263.62	229.54	349.5484459
71	71.10	181.16	23.07	498.56	212.35	541.8990645
71	71.11	178.34	43.51	479.59	455.29	661.2832617
71	71.12	222.36	34.67	639.17	442.08	777.1570081
71	71.13	215.38	36.74	643.03	480.07	802.4679344
71	71.14	215.49	34.31	544.59	371.64	659.313702
71	71.15	196.71	36.63	314.24	233.61	391.5615018
71	71.16	159.33	46.21	348.23	363.22	503.1827713
71	71.17	189.57	47.87	241.8	267.34	360.4690217
72	72.1	346.25	25.8	71.14	34.39	79.01627491
72	72.2	36.06	19.88	76.35	27.61	81.18888224
72	72.3	74.75	59.4	79.42	134.28	156.0085087
72	72.4	28.03	51.7	74.89	94.84	120.8434429
73	73.1	221.97	74.38	582.17	1092.44	1237.880068
73	73.2	222.89	49.05	125.18	144.26	190.9999476
73	73.3	191.01	27.03	187.89	95.87	210.9353195
73	73.4	205.95	55.03	163.97	234.39	286.0504029
73	73.5	189.38	5.75	207.43	20.88	208.4782466
73	73.6	235.66	48.59	486.42	551.6	735.436589
73	73.7	234.06	57.07	481.59	743.51	885.8532882
73	73.8	219.31	66.86	307.64	719.88	782.8598751
73	73.9	208.1	64.41	503.29	1051.12	1165.398678
73	73.10	242.21	69.49	275.39	735.99	785.825001
73	73.11	255.4	33.68	229.67	153.06	275.9994067

Continued

73	73.12	240.78	40.89	202.76	175.59	268.2227912
74	74.1	186.26	69.51	294.25	787.25	840.4437072
74	74.2	163.68	59.63	316.48	540.06	625.9587798
74	74.3	192.88	63.56	318.85	641.31	716.2009764
74	74.4	189.58	53.83	343.17	469.48	581.5299814
74	74.5	173.22	55.53	295.75	430.81	522.5565219
74	74.6	184.28	52.05	204.37	262.1	332.3605074
74	74.7	174.87	37.98	144.83	113.05	183.7281454
74	74.8	166.33	48.49	163.53	184.77	246.742809
74	74.9	163.14	42.55	196.91	180.77	267.3038365
75	75.1	19.89	39.82	89.33	74.48	116.3061447
75	75.2	7.29	72.23	103.04	321.52	337.6275344
75	75.3	337.3	6.44	119.83	13.52	120.5902952
77	77.1	24.06	78.09	111.32	349.49	366.7906794
77	77.2	40.36	15.37	97.33	26.76	100.9416985
77	77.3	13.66	71.22	89.35	262.8	277.5738866
77	77.4	27.07	77.34	71.89	319.92	327.8978172
77	77.5	46.86	10.92	57.41	11.07	58.467538
77	77.6	16.92	58.74	79.01	130.17	152.2721544
77	77.7	19.61	42.24	73.97	67.17	99.9168144
78	78.1	9.21	49.86	305.1	361.87	473.3243
78	78.2	340.53	35.32	268.15	190.02	328.6518263
78	78.3	24.68	2.71	145.45	6.87	145.612154
78	78.4	34.23	25.09	273.15	127.89	301.606987
78	78.5	358.03	39.92	262.5	219.65	342.2752876
78	78.6	4.75	51.46	235.29	295.36	377.6227134
78	78.7	8.67	37.66	200.57	154.81	253.3662586
78	78.8	20.07	29.39	178.92	100.76	205.3410431
78	78.9	42.75	14.33	217.07	55.47	224.0453209
78	78.10	33.28	23.61	224.91	98.32	245.4614644
78	78.11	19.83	23.97	216.33	96.16	236.7391275
78	78.12	26.39	0.04	162.44	0.11	162.4400372
79	79.1	343.75	8.84	379.39	59.03	383.954832
79	79.2	19.14	17.91	436.52	141.07	458.7487932
79	79.3	41.33	34.39	448.77	307.21	543.8497007
79	79.4	16.16	35.19	486.51	343.13	595.3403875
79	79.5	5.57	33.14	390.25	254.78	466.0556951
79	79.6	27.97	6.05	195.57	20.73	196.6655989

Continued

79	79.7	3.2	6.58	246.54	28.44	248.1749488
79	79.8	5.94	19.78	543.74	195.59	577.8482809
79	79.9	1.68	23.09	833.23	355.26	905.8045598
79	79.10	24.14	29.95	551.4	317.72	636.3866422
80	80.1	202.11	64.07	161.26	331.62	368.7500671
80	80.2	180.6	62.05	203.39	383.38	433.9904567
80	80.3	205.96	44.1	479.23	464.45	667.3643648
80	80.4	196.39	43.63	758.83	723.31	1048.332163
80	80.5	184.23	45.01	435.81	435.9	616.3920555
80	80.6	177.96	50.34	210.26	253.66	329.4733118
80	80.7	199.04	61.13	91.9	166.68	190.3361038
80	80.8	195.97	55.55	174.04	253.7	307.6582708
80	80.9	191.7	54.22	141.35	196.12	241.7496161
80	80.10	179.83	54.03	100.84	138.97	171.7013876
80	80.11	181.59	54.14	59.09	81.74	100.861567
81	81.1	285.1	14.28	999.41	254.3	1031.255952
81	81.2	24.28	31.1	1126.28	679.36	1315.308575
81	81.3	52.14	34.89	802.81	559.8	978.7134086
81	81.4	32.76	16.76	492.37	148.25	514.2045113
81	81.5	58.98	37.88	733.32	570.45	929.0701937
81	81.6	28.23	35.1	948.79	666.93	1159.740527
81	81.7	38.18	37.12	969.13	733.39	1215.34927
81	81.8	19.98	39.63	722.14	598.05	937.6299814
81	81.9	14.95	16.98	490.2	149.68	512.5428201
82	82.1	267.56	24.53	278.28	127	305.8901084
82	82.2	269.84	27.74	392.26	206.32	443.2108415
82	82.3	257.46	27.92	491.27	260.32	555.9790601
82	82.4	237.83	25.86	631.44	306.03	701.6914097
82	82.5	237.25	24.67	860.26	395.16	946.6777135
82	82.6	230.86	29.16	763.97	426.31	874.8659194
82	82.7	264.32	35.58	655.88	469.22	806.4403157
82	82.8	91.02	40.97	586.83	509.54	777.1746654
82	82.9	255.2	35.27	719.68	509.05	881.5164235
82	82.10	255.76	30.63	708.36	419.45	823.2327691
83	83.1	218.11	68.73	85.43	219.49	235.5294992
83	83.2	189.7	74.34	112.83	402.47	417.9864948
83	83.3	192.43	69.69	116.58	315.03	335.9089122
83	83.4	185.52	69.43	134.03	357.06	381.3867912

Continued

83	83.5	146.37	50.69	138.42	169.07	218.5057466
83	83.6	182.83	72.5	84.93	269.4	282.4702903
84	84.1	52.19	31.72	578.69	357.74	680.3381686
84	84.2	48.68	31.99	546.67	341.45	644.5433976
84	84.3	41.08	32.45	640	406.99	758.4463462
84	84.4	28.06	26.43	565.7	281.12	631.7000431
84	84.5	10.54	23.19	560	239.93	609.2342775
84	84.6	24.04	30.09	425.8	246.73	492.1192263
84	84.7	341.34	32.29	338.1	213.69	399.9687814
86	86.1	203.37	2.15	180.03	6.75	180.156497
86	86.2	204.23	6.1	232.03	24.79	233.3505196
86	86.3	153.44	11.66	271.26	55.95	276.9700166
86	86.4	190.81	22.18	271.83	110.84	293.5592862
86	86.5	157.2	38.35	395.31	312.8	504.0970503
86	86.6	153.74	39.33	383.5	314.24	495.8013994
86	86.7	184.73	33.44	465.58	307.43	557.9228811
86	86.8	171.56	32.38	414.27	262.69	490.5361037
86	86.9	171.43	35.32	292.91	207.52	358.971891
86	86.10	169.46	16.76	462.65	139.35	483.1805511
86	86.11	156.39	31.94	320.27	199.67	377.4135422
86	86.12	167.19	27.69	328.13	172.22	370.5793104
86	86.13	168.27	14.94	321.23	85.71	332.4679188
86	86.14	172.37	28.34	291.66	157.33	331.3884194
86	86.15	175.44	12.78	294.95	66.92	302.4463405
86	86.16	183.55	14.37	319.97	81.96	330.3002309
86	86.17	186.24	14.83	412.45	109.24	426.6712787
86	86.18	165.12	12.69	270.73	60.95	277.5060998
87	87.1	152.16	26.67	843.33	423.57	943.7250838
87	87.2	174.32	51.22	961.47	1196.73	1535.117993
87	87.3	165.35	57.22	1066.19	1655.47	1969.096757
87	87.4	160.98	53.02	1264	1678.33	2101.068202
87	87.5	153.88	56.45	1534.64	2314.6	2777.137571
87	87.6	142.31	46.71	2088.77	2217.55	3046.389357
87	87.7	181.77	57.18	1929.79	2991.9	3560.274576
87	87.8	172.23	57.61	1751.5	2760.49	3269.259441
87	87.9	171.91	62.59	1438.19	2773.42	3124.139717
87	87.10	164.77	68.04	1487.48	3688.15	3976.813696
87	87.11	163.94	67.52	1678.52	4056.29	4389.865369

Continued

87	87.12	164.89	64.99	1975.67	4235.36	4673.494012
87	87.13	166.14	60.74	2173.96	3881.07	4448.46113
87	87.14	165.26	63.8	1912.82	3886.81	4331.994036
87	87.15	165.03	67.45	1662.17	4003.85	4335.16135
87	87.16	166.66	68.05	1451.17	3600.93	3882.343523
87	87.17	163.68	66.83	1324.07	3094.44	3365.816436
87	87.18	159.58	63.73	1375.59	2786.72	3107.741335
87	87.19	161.56	58.8	1614.61	2666.55	3117.283169
87	87.20	171.73	49.52	1832.88	2147.33	2823.203008
87	87.21	165.07	33.98	1965.33	1324.64	2370.061843
87	87.22	175.75	40.96	2154.23	1870.26	2852.819546
87	87.23	253.44	37.66	1885.4	1455.18	2381.655305
88	88.1	280.64	75.54	662.97	2570.58	2654.695982
88	88.2	285.56	72.18	826.12	2570.58	2700.065886
88	88.3	280.06	69.68	952.11	2570.58	2741.239681
88	88.4	88.37	64.91	1239.15	2646.02	2921.799884
88	88.5	87.08	72.25	913.39	2853.5	2996.121416
88	88.6	83.58	76.22	666.39	2718.13	2798.625793
88	88.7	270.68	67.08	1127.69	2666.72	2895.354951
88	88.8	89.6	70.63	937.64	2666.72	2826.758626
88	88.9	86.16	80.27	457.12	2666.72	2705.615319
88	88.10	79.04	75.86	671.81	2666.72	2750.04077
88	88.11	61.56	77.59	586.77	2666.72	2730.511782
88	88.12	60.82	46.71	895.49	950.68	1306.022512
88	88.13	47.66	21.41	1304.22	511.32	1400.870426
88	88.14	43.29	45.4	1373.08	1392.43	1955.558741
88	88.15	44.71	37.55	1808.95	1390.81	2281.809054
88	88.16	49.43	35.4	1975.6	1403.88	2423.607727
88	88.17	59.53	38.82	1763.5	1418.99	2263.507206
88	88.18	79.61	48.37	1261.34	1418.99	1898.555034
88	88.19	75.24	57.32	888.3	1384.74	1645.169219
88	88.20	83	55.85	939.14	1384.42	1672.902471
88	88.21	270.09	59.27	823.11	1384.42	1610.629942
88	88.22	272.53	60.52	782.65	1384.42	1590.333223
88	88.23	85.14	60.45	784.71	1384.42	1591.34802
88	88.24	65.55	49.05	974.3	1122.81	1486.594358
88	88.25	59.5	16.51	1140.53	337.95	1189.545663
88	88.26	60.83	12.44	1081.26	238.58	1107.268533

Continued

88	88.27	66.48	4.41	867.21	66.85	869.7827928
88	88.28	51.15	18.68	717.13	242.4	756.9895619
88	88.29	55.51	31.84	596.94	370.77	702.7145626
88	88.30	57.04	48.03	434.23	482.73	649.2949606
88	88.31	45.91	46.71	605.4	642.62	882.8757695
88	88.32	41.23	39.85	827.26	690.54	1077.592037
89	89.1	0.9	23.13	125.55	53.62	136.5207197
89	89.2	31.3	39.53	139.12	114.82	180.3829449
89	89.3	60.79	14.41	163.63	42.04	168.9441875
89	89.4	38.79	36.33	231.54	170.25	287.3949097
89	89.5	21.25	8.84	238.78	37.13	241.649592
89	89.6	25.49	24.22	302.15	135.92	331.3138526
89	89.7	10.08	9.7	289.49	49.48	293.6881518
89	89.8	346.1	7.46	388.44	50.84	391.7529058
89	89.9	6.59	15.86	724.15	205.78	752.8204506
89	89.10	15.88	18.73	683.48	231.71	721.6885994
89	89.11	4.88	26.22	657.92	324.09	733.4119269
89	89.12	344.85	25.04	763.73	356.82	842.9733242
89	89.13	35.93	22.47	870.74	360.2	942.3015375
89	89.14	20.89	10.94	621.04	120.09	632.5442986
89	89.15	338.65	3.28	588.17	33.75	589.1375148
89	89.16	5.47	10.1	606.21	107.99	615.7535255
89	89.17	26.79	11.49	440.28	89.47	449.27871
89	89.18	23.91	11.56	332.97	68.13	339.8686773
90	90.1	15.67	13.76	224.01	54.84	230.6250327
90	90.2	15.47	29.01	196.03	108.7	224.1505095
90	90.3	15.16	36.64	128.33	95.43	159.9233373
90	90.4	345.96	24.97	161.51	75.2	178.1586936
90	90.5	46.36	61.91	124.16	232.63	263.6900121
90	90.6	38.11	42.94	239.39	222.76	327.0009017
90	90.7	31.7	5.11	202.98	18.14	203.7889595
91	91.1	10.33	34.03	157.03	106.05	189.486209
91	91.2	18.72	34.71	317.93	220.23	386.7566907
91	91.3	1.57	45.02	403.82	404.13	571.3069659
91	91.4	354.11	42.96	744.83	693.63	1017.78893
91	91.5	7.18	39.83	1104.53	921.31	1438.331894
91	91.6	12.2	39.11	1291.51	1049.79	1664.348859
91	91.7	9.1	23.11	1568.02	669.18	1704.842689

Continued

91	91.8	15.25	33.65	1389.94	925.23	1669.725653
91	91.9	24.42	33.7	1063.06	708.96	1277.779654
91	91.10	23.56	25.05	848.62	396.56	936.704723
91	91.11	339.07	28.3	609.14	327.96	691.8159446
91	91.12	339.81	47.47	604.95	659.45	894.8959744
91	91.13	342.39	49.93	694.9	826.08	1079.487923
92	92.1	20.53	4.98	352.47	30.69	353.8035853
92	92.2	5.5	39.04	315.04	255.44	405.5857433
92	92.3	48.87	30.77	487.22	290.08	567.0359202
92	92.4	21.28	39.77	856.85	713.12	1114.778927
92	92.5	50.48	50.3	774.83	933.36	1213.063238
92	92.6	30.15	42.23	860.5	781.05	1162.109871
92	92.7	56.92	43.11	1162.82	1088.6	1592.859163
92	92.8	30.3	54.29	860.18	1196.57	1473.665294
92	92.9	28.4	48.06	1072.59	1193.62	1604.736119
92	92.10	18.52	38.43	1763.81	1399.33	2251.477329
92	92.11	56.37	22.54	1964.29	815.33	2126.781186
92	92.12	45.05	27.46	1472.72	765.37	1659.727518
92	92.13	20.57	24.9	1379.78	640.6	1521.236736
92	92.14	37.1	24.14	1529.18	685.27	1675.704761
92	92.15	35.08	26.52	1049.94	523.93	1173.403873
92	92.16	32.04	29.44	856.72	483.45	983.7139121
92	92.17	351.19	20.04	721.65	263.25	768.1661832
92	92.18	15.69	27.98	617.14	327.93	698.8561114
92	92.19	17.21	27.4	548.93	284.5	618.2753391
92	92.20	15.65	28.88	432.78	238.71	494.2479059
92	92.21	21.25	17.95	330.56	107.09	347.4740015
93	93.1	47.15	52.25	495.31	639.6	808.9623947
93	93.2	38.64	29.46	679.03	383.6	779.8914674
93	93.3	37.6	28.59	738.46	402.46	841.0096451
93	93.4	79.83	28.25	711.8	382.48	808.0533339
93	93.5	28.09	35.85	576.26	416.36	710.9368729
93	93.6	34.43	31.68	382.86	236.32	449.9210175
93	93.7	19.82	37.87	221.03	171.85	279.9762193
94	94.1	8.47	49.97	978.44	1164.93	1521.317435
94	94.2	29.24	58.52	1020.06	1665.71	1953.231222
94	94.3	349.24	48.98	913.64	1050.46	1392.194046
94	94.4	28.18	54.36	705.42	983.88	1210.635053

Continued

94	94.5	40.86	56.85	710.56	1088.08	1299.543612
94	94.6	14.55	49.53	677.95	794.69	1044.580489
94	94.7	28.88	44.1	644.38	624.36	897.2463396
94	94.8	43.95	38.54	771.71	614.81	986.675053
94	94.9	67.68	38.57	440.57	351.35	563.5146381
94	94.10	44.54	38.65	255.64	204.45	327.3402085
94	94.11	14.26	26.91	402.84	204.47	451.7610502
94	94.12	32.03	43.3	356.28	335.69	489.5132424
94	94.13	0.24	59.15	304.42	509.72	593.7053266
94	94.14	16.28	49.62	462.82	544.22	714.4072794
94	94.15	359.03	36.96	615.95	463.42	770.8128819
94	94.16	337.13	46.27	433.59	453.26	627.2518758
94	94.17	356.38	32.2	291.97	183.88	345.0483086
94	94.18	12.34	37	449.66	338.86	563.0454824
94	94.19	359.13	36.37	336.82	248.06	418.3078723
94	94.20	22.8	13.02	340.91	78.81	349.9009063
94	94.21	63.14	1	451.05	7.86	451.118479
94	94.22	30.86	13.67	407.52	99.08	419.3916985
94	94.23	24.5	6.88	389.8	47	392.62328
95	95.1	20.14	44.72	109.32	108.26	153.8541192
95	95.2	13.86	34.22	113.74	77.37	137.5605485
95	95.3	19.33	23.55	180.36	78.6	196.742699
95	95.4	3.12	34.39	480.15	328.69	581.8772539
95	95.5	358.41	40.91	399.41	346.07	528.4815919
95	95.6	18.13	55.97	293.73	434.95	524.8417051
95	95.7	28.37	50.88	320.47	394.01	507.882763
95	95.8	29.19	36.25	306.58	224.8	380.1661958
95	95.9	33.63	25.39	366.37	173.89	405.5424873
95	95.10	41.45	28.23	413.73	222.14	469.5941785
95	95.11	0.19	11.33	300.11	60.14	306.0765128
95	95.12	354.9	13.09	326.57	75.93	335.2809714
95	95.13	4.29	29.63	347.2	197.51	399.4471681
95	95.14	35.55	1.73	312.99	9.44	313.1323262
95	95.15	31.14	34.46	310.22	212.93	376.2653762
95	95.16	25.61	21.59	331	130.95	355.9619397
95	95.17	32.53	0.69	302.81	3.63	302.8317569
95	95.18	6.41	1.63	336.97	9.56	337.1055836
95	95.19	12.6	7.79	635.51	86.92	641.4265714

Continued

95	95.20	13.96	8.95	808.24	127.27	818.1989676
95	95.21	11.07	22.33	901.33	370.21	974.397872
95	95.22	357.17	33.53	821.44	544.36	985.439741
95	95.23	5.51	38.2	738.5	581.24	939.7990145
95	95.24	13.24	39.4	705.55	579.52	913.0412
95	95.25	6.04	37.38	686.36	524.44	863.7866422
95	95.26	355.98	33.04	693	450.74	826.689511
95	95.27	2.63	36.64	812.57	604.35	1012.674147
95	95.28	6.79	35.61	958.15	686.22	1178.536937
95	95.29	9.6	35.54	878.46	627.53	1079.57671
95	95.30	11.58	29.92	853.38	491.06	984.5797824
95	95.31	2.39	30.67	814.56	483.04	947.0140628
95	95.32	359.55	22.59	725.81	302.03	786.1439289
95	95.33	346.51	25.2	678.7	319.39	750.0957686
95	95.34	350.14	35.08	670.54	470.87	819.3548978
95	95.35	19.83	44.81	621.49	617.32	875.9759143
96	96.1	194.85	27.04	230.77	117.77	259.0840902
96	96.2	222.27	31.27	315.57	191.68	369.2230319
96	96.3	207.98	36.21	491.35	359.79	608.9939791
96	96.4	203.72	27.83	713.77	376.86	807.149969
96	96.5	212.06	29.62	662.11	376.48	761.6605822
96	96.6	208.53	23.19	845.01	362.01	919.2894757
96	96.7	181.57	25.56	760.07	363.58	842.5537498
96	96.8	195.68	23.05	727.6	309.55	790.7104163
96	96.9	222.55	18.03	704.95	229.51	741.3699094
96	96.10	198.73	19.91	780.2	282.62	829.8108847
96	96.11	186.25	26.41	687.2	341.28	767.2782275
96	96.12	183.26	26.98	689.45	351.05	773.6778432
96	96.13	200.64	23.34	592.18	255.54	644.9634439
96	96.14	186.33	41.9	252.48	226.56	339.2279234
96	96.15	195.19	55.61	205.85	300.76	364.4596001
96	96.16	192.08	40.6	249.49	213.81	328.5726346
97	97.1	177.71	14.93	1304.53	347.73	1350.079506
97	97.2	189.02	22.97	1215.69	515.32	1320.400272
97	97.3	192.5	28.39	1137.03	614.61	1292.510222
97	97.4	177.87	28.97	1123.03	621.77	1283.664409
97	97.5	164.6	23.24	943.53	405.15	1026.837564
97	97.6	184.31	20.96	740.97	283.9	793.4959048

Continued

97	97.7	184.13	28.11	772.25	412.52	875.5243074
97	97.8	207.2	29.69	803.28	457.91	924.6298321
97	97.9	205.91	29.32	864.07	485.2	990.9772979
97	97.10	231.75	39.15	478.54	389.64	617.1060372
97	97.11	197.45	12.18	394.56	85.16	403.6456604
97	97.12	190.77	19.46	298.01	105.32	316.0731917
97	97.13	199.15	33.08	169.71	110.55	202.540827
97	97.14	171.94	27.9	117.92	62.45	133.4358606
98	98.1	203.5	70.53	41.99	118.78	125.9835247